Combined protein and transcript single cell RNA sequencing reveals cardiovascular disease and HIV signatures

Jenifer Vallejo, Ryosuke Saigusa (equal contribution) et al.

Short title: Human CVD signatures by single cell RNA-Seq

Corresponding Author
Klaus Ley, MD
La Jolla Institute for Immunology
9420 Athena Circle
La Jolla, CA 92037, USA
(858) 752-6661 (tel)
(858) 752-6985 (fax)
klaus@lji.org

Total word count: 12257

Abstract

Background. HIV-infected people have an increased risk of atherosclerosis-based cardiovascular disease (CVD), even when the HIV virus is fully controlled. Both chronic HIV infection and CVD are chronic inflammatory diseases. The interaction between these two diseases is not well understood.

Methods. The Women's Interagency HIV Study (WIHS) collected peripheral blood mononuclear cells (PBMCs) and data on subclinical CVD defined by carotid artery ultrasound from HIV-infected women. We interrogated 32 PBMC samples using combined protein and transcript panel single cell (sc) RNA sequencing of women without HIV or CVD, with HIV only, with HIV and CVD, and with HIV and CVD treated with cholesterol-lowering drugs. Expression of 40 surface markers enabled detailed analysis of all major cell types, resolving 58 clusters in almost 42,000 single cells.

Results. Many clusters including 5 of 8 classical monocyte clusters showed significantly different gene expression between the groups of participants, revealing the inflammatory signatures of HIV, CVD and their interactions. Genes highly upregulated by CVD included CCL3, CCL4 and IL-32, whereas CXCL2 and 3 were more highly upregulated by HIV. Many genes were synergistically upregulated by HIV and CVD, but others were antagonistically regulated, revealing that the gene signature in people with HIV and CVD is not simply the sum of the HIV and CVD signatures. Elevated expression of most inflammatory genes was reversed by cholesterol control (statin treatment). The cell numbers in 3 of 5 intermediate monocyte subsets, 1 of 14 CD8 T cell subsets, 1 of 6 B cell subsets and 1 of 6 NK cell subsets showed significant changes with HIV or CVD.

Conclusions. We conclude that HIV and CVD show interactive inflammatory signatures including chemokines and cytokines that are improved by cholesterol-lowering drugs.

Keywords: CVD, HIV, scRNA-seq, transcriptomes, surface markers, antibodies, PBMC, human, cholesterol-lowering drugs.

Introduction

Most people living with HIV, including the Women's Interagency HIV Study (WIHS) participants, are on antiretroviral therapy (ART), leading to low or undetectable HIV viral loads[1]. Nevertheless, low-level systemic inflammation remains measurable.[2] Chronic inflammation is thought to drive morbidity and mortality in people living with HIV, much of it from sequelae of cardiovascular disease (CVD).[3,4] Cardiovascular risk in people living with HIV is elevated ~3-fold compared to uninfected controls.[5,6] Within the next 10 years, it is expected that 78% of people living with HIV will be diagnosed with CVD.[7,8] How persistent inflammation in chronic HIV infection drives CVD is not known. Predicting the prognosis or monitoring the efficacy of therapies remains challenging.

Prior studies characterized peripheral blood mononuclear cells (PBMCs) in HIV-infected people and uninfected controls using flow cytometry or mass cytometry. Other than the well-known loss of CD4 T cells in HIV infection[9] and their rebound with ART,[10] changes were noted in monocytes and natural killer (NK) cells.[11] Among people living with HIV, those with CVD showed a loss of CXCR4 expression in nonclassical monocytes (NCM).[12] Other studies reported an association between monocytes and coronary artery calcium progression in people living with HIV[13], persistent activation of classical monocytes (CM),[14,15] changes in NK cells,[11,16–22] CD8 T cells[23–26] and B cells.[27–32]

WIHS is an ongoing multi-center, prospective, observational cohort study of over 4,000 women with or at risk of HIV infection that was initiated in 1994. Almost all WIHS participants with HIV are on ART. PBMCs were cryopreserved and shipped on liquid N_2, following strict standard operating procedures that ensured preservation of cell surface phenotype, viability and transcriptomes.[33] PBMCs can be analyzed without mechanical or enzymatic dissociation, which are known to alter cell surface markers and transcriptomes.[34] PBMC are attractive for single cell RNA sequencing (scRNA-Seq) studies, because they are available in many clinical studies of specific populations with defined diseases and outcomes. The participants sampled for the present study were part of a substudy nested within the WIHS,[35,36] which provided detailed

information on subclinical atherosclerosis. Participants underwent high-resolution B-mode carotid artery ultrasound to image six locations in the right carotid artery.[37]

scRNA-Seq has been applied to human PBMCs in diseases including cancers,[38–41] inflammatory bowel disease[42,43] and autoimmune disease[44,45]. One study reported the effect of acute HIV infection on PBMC transcriptomes[46]. No single cell studies of PBMCs of people living with chronic HIV infection and CVD have been reported.

Here, we report transcriptomes and cell surface phenotypes of almost 42,000 PBMCs from 31 participants of the WIHS study at unprecedented resolution. We used the targeted scRNA-Seq BD Rhapsody platform[47,48] that simultaneously provides surface phenotype (40 mAbs) and transcriptomes (485 immune and inflammatory transcripts) in the same cells. We compared non-HIV non-CVD with HIV+ women (HIV effect), HIV+ women with and without subclinical cardiovascular disease as assessed by carotid ultrasound (CVD effect) and the effect of treatment with cholesterol-lowering drugs (statin effect). Hundreds of genes in tens of clusters were significantly differentially expressed between the disease groups. Six of 58 resolved PBMC clusters showed significant changes in cell proportions specific for HIV or CVD.

Results

Population and cells.

The 32 WIHS participants studied were aged 47-62, all (ex)smokers, most African American or Hispanic. Matched groups of 8 women each were selected for subclinical CVD and HIV status: CVD-HIV- (non-CVD non-HIV); CVD-HIV+ (living with HIV); CVD+HIV+statin- (living with HIV, evidence of CVD); CVD+HIV+statin+ (living with HIV, evidence of CVD, treated with cholesterol-lowering drugs) (**Table S1**). PBMC tubes were shipped from the central repository on liquid N_2, thawed and processed according to standard operating procedures. Cell viability was 88±5% (**Table S2**). To avoid batch effects, all cells were hash-tagged for multiplexing, with 4 samples run per 250,000-well plate (total of 8 plates). The pooled cells were labeled with 40 titrated oligonucleotide-tagged mAbs (**Table S3**). After quality controls and three-stage doublet removal, 41,611 single cell transcriptomes from 31 WIHS participants (one sample was lost in hash tagging) were successfully analyzed (**Table S4**). An overview of the experimental design and workflow is shown in **Figure S1**.

Surface marker-based cell identification.

In combined protein and transcript panel single cell sequencing, just like in CITE-Seq,[49] REAP-Seq[50] or flow cytometry, non-specific binding contributes to the antibody signal, in part, because Fc block is not complete.[51,52] The type and number of Fc receptors varies among cell types, causing different levels of background for the same antibody in different cell types.[53–56] Additional background is caused by unbound oligonucleotide-tagged antibody remaining in the nanowell that will be amplified and sequenced.[48] To account for all sources of background, we gated based on biaxial plots of mutually exclusive markers. This yielded thresholds for all 40 markers used (**Table S5**). After thresholding, we used Boolean gating on surface markers to readily identify known cell types to the satisfaction of experts in the field. An alternative to surface marker-based cell calling is integrated analysis by surface markers and transcripts using Seurat.[57,58] (**Figure S2**).

Correlation between gene and cell surface marker expression.

In immunology, surface markers are widely used to define and distinguish cell types.[59–62] The correlation between cell surface protein and mRNA expression is weak in immune cells.[63] Therefore, scRNA-Seq without surface phenotype information has led to much frustration in the field, because the expression of many genes encoding well-known surface markers remains undetected in scRNA-Seq.[59,64,65] It is still difficult to call cell types based on gene expression data alone, which emphasizes the need for cell surface phenotypes in addition to transcriptomes. Here, we correlated gene expression with cell surface expression for 41 pairs of genes and proteins **(Table S6)**. For most markers, we confirm weak correlations[63], which illustrates the value of monitoring cell surface phenotype in scRNA-Seq.

Major cell types.

T, B, NK cells and monocytes were identified by 8 antibody markers using biaxial gating, corresponding to established gating schemes for human PBMCs.[66–68] CD3 and CD19 expression are mutually exclusive and specific for T and B cells, respectively (**Figure S3**). Thus, we identified CD4 (**Figure S4A**) and CD8 T cells (**Figure S4B**), classical, nonclassical and intermediate monocytes (**Figure S4C**), B cells (**Figure S4D**), and natural killer (NK) cells (**Figure S4E**).[69–71]

Subclustering.

Each major cell type (**Figure 1**, center) was subclustered by all expressed surface markers (**Table S7**) using UMAP and Louvain[72] clustering (**Figure 1**). Gates were overlaid and used in all subsequent UMAP figures (cell numbers in **Table S8)**. Violin plots of surface marker distribution of each cluster in **figure S5**.

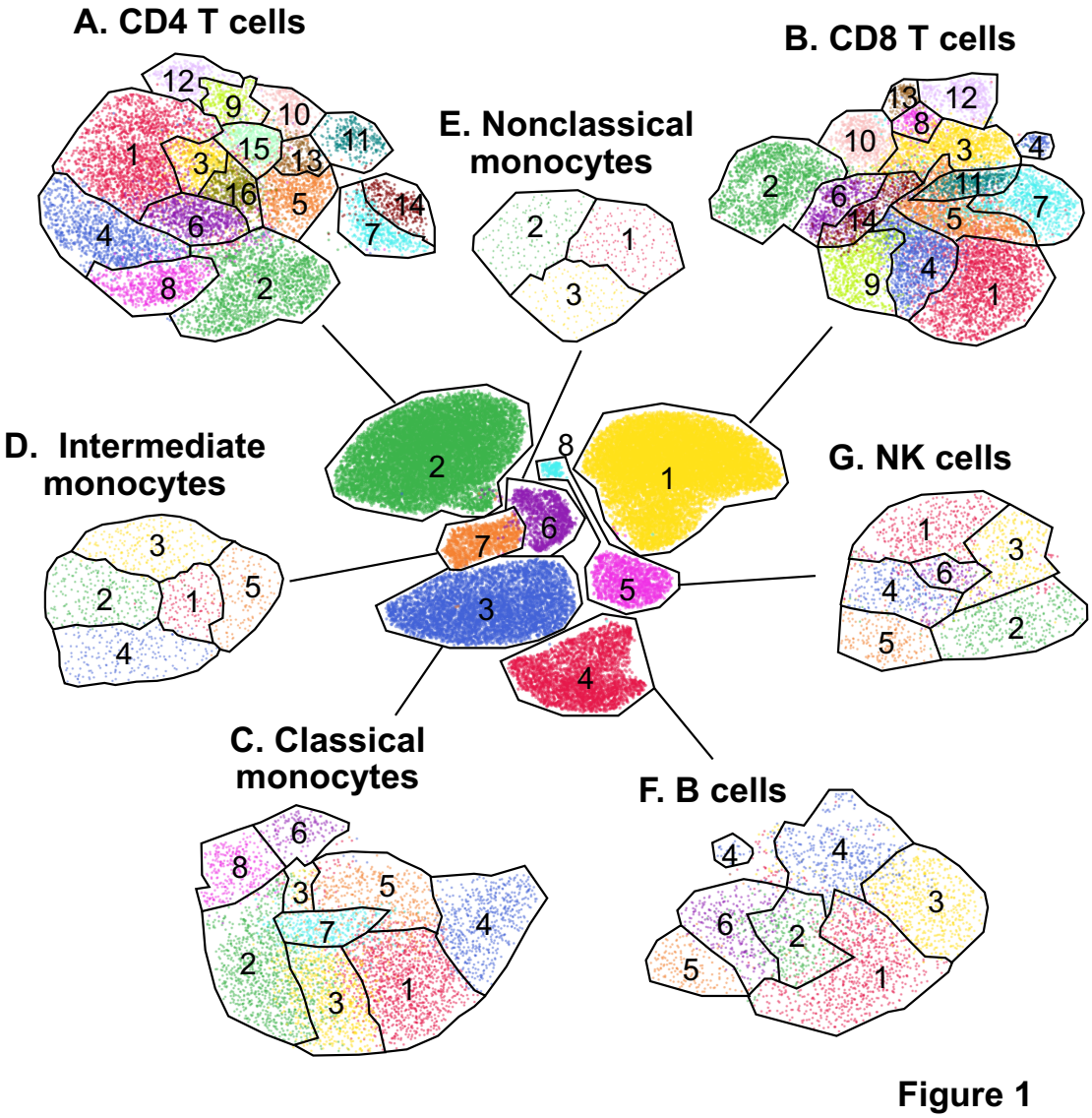

Figure 1. Antibody- based UMAP clustering of major cell types. The major known cell types were UMAP-Louvain-clustered by CD3, CD19, CD14, CD16 and CD56 surface expression (central panel). Then, each major known cell type was UMAP-Louvain-clustered by all non-negative surface markers (see table S7 for list). **(A) CD4 T cells** formed 16 clusters, cluster numbers indicated; **(B) CD8 T cells** formed 14 clusters; **(C) Classical monocytes (CM)** formed 8, **(D) Intermediate monocytes (INT)** 5 and **(E) Nonclassical monocytes (NCM)** 3 clusters. **(F) B cells and (G) NK cells** formed 6 clusters each.

Among CD4 T cells (**Figure 2A**), CD2, the ligand for CD48 and CD58, was expressed in almost all cells, as expected. The high affinity IL2 receptor IL2RA (CD25) was expressed in about a third of the CD4 T cells and was strikingly high in cluster 13, which was also low for IL7 receptor (CD127), defining regulatory T cells (Tregs).[73,74] CD45RA and RO were mutually exclusive,

separating naive and antigen-experienced CD4 T cells. CXCR3 (CD183) identifies T-helper-1 (Th1) cells in human PBMCs[75] and was highly expressed in clusters 6, 14 and 16. Cluster 14 co-expressed CXCR5 (CD185) with CXCR3. Cluster 7 expressed CXCR5 as the only chemokine receptor, suggesting it may contain follicular helper (TFH) T cells. Based on surface marker information, all CD4 T cell clusters were called (**Figure 3A**).

CD8 T cells. All CD8 T cells expressed CD2 (**Figure 2B**). Cluster 3 exclusively expressed CD9 and CD36, identifying these cells as NK-like CD8 cells.[76,77] Clusters 7 and 13 were identified as NK-like T cells with a CD45RA+ terminally differentiated memory (EMRA) phenotype. Based on these markers, all CD8 T cell clusters were called (**Figure 3B**).

Monocytes (**Figure 2C**). As expected, all **classical monocytes (CM)** were CD11b+ (**Figure 2C**). There were gradients of CD9[78], CD69, CD137, CD142 (tissue factor) and CD163 (hemoglobin-haptoglobin receptor) expression. The scavenger receptor CD36 and the antigen presentation co-receptor CD86 were expressed in all classical monocytes. As expected, the chemokine receptor CCR2 was expressed in all classical monocytes. Based on these markers, 5 of the 8 classical monocyte subsets were called (**Figure 2C**) and related to subsets described by mass cytometry.[78] **Intermediate CD14+CD16+ monocytes (INT)** have been considered pro-inflammatory by several investigators[79–83] and are known to be increased in people with HIV[84,85] and with CVD.[82,86,87] All intermediate monocytes highly expressed the inflammation-induced costimulatory molecule CD86 (**Figure 2C**). Cluster INT3 highly expressed CD142 (tissue factor), which has previously been implicated in people living with HIV.[14] Since subsets of intermediate monocytes have not been described before, we propose a provisional naming suggestion (**Figure 3C**). **Nonclassical monocytes (NCM)** are considered anti-inflammatory.[88] In this study, they formed 3 clusters (**Figure 2C**). Strikingly, expression of CD9 and CD36 was limited to cluster 3,

1 suggesting that this cluster corresponds to the previously described CD9+CD36+ NCM.[78] CD11c,

2 CD74[78], CD86 and CD141 were expressed in all NCMs (**Figure 3C)**.

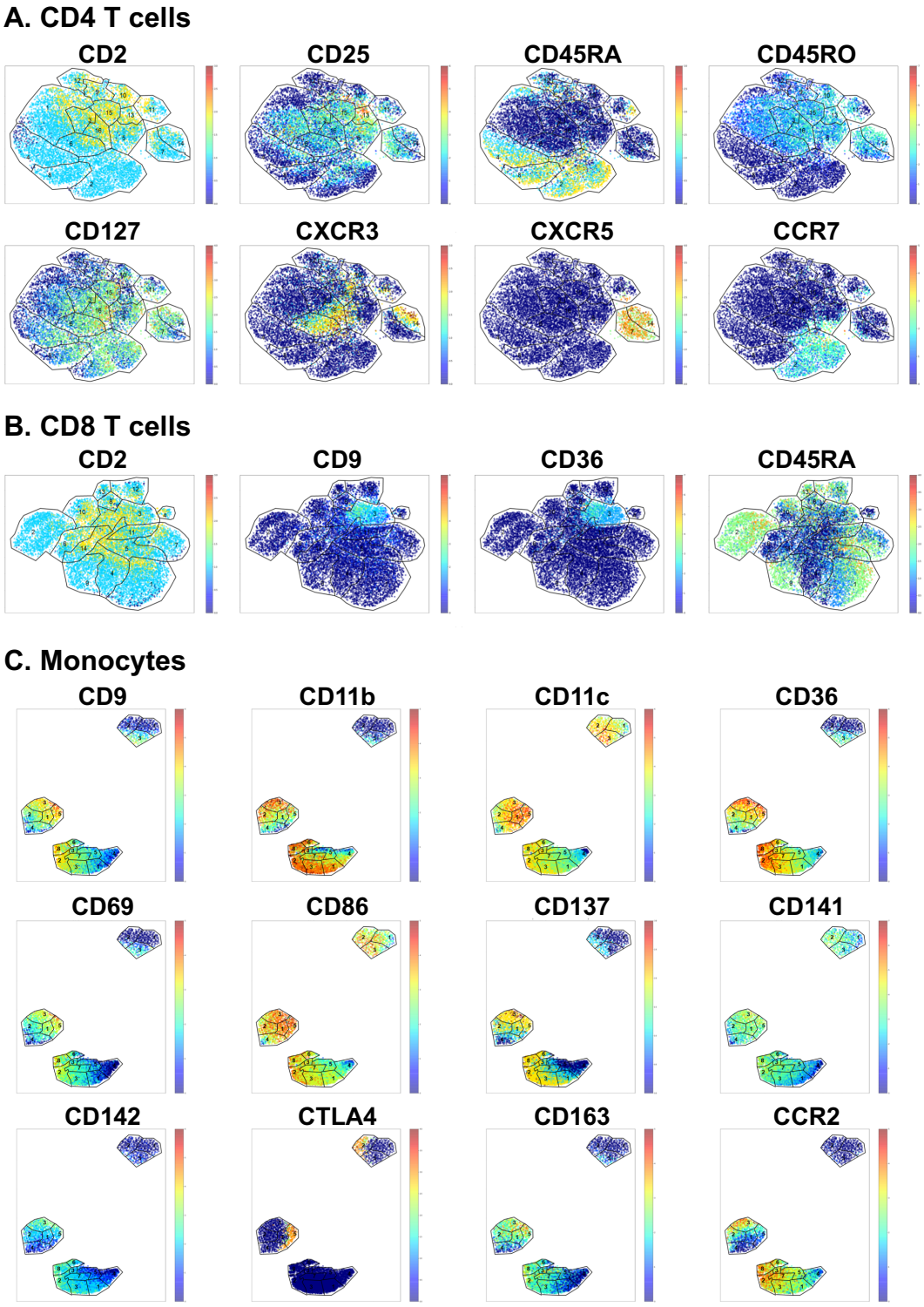

3 **Figure 2**

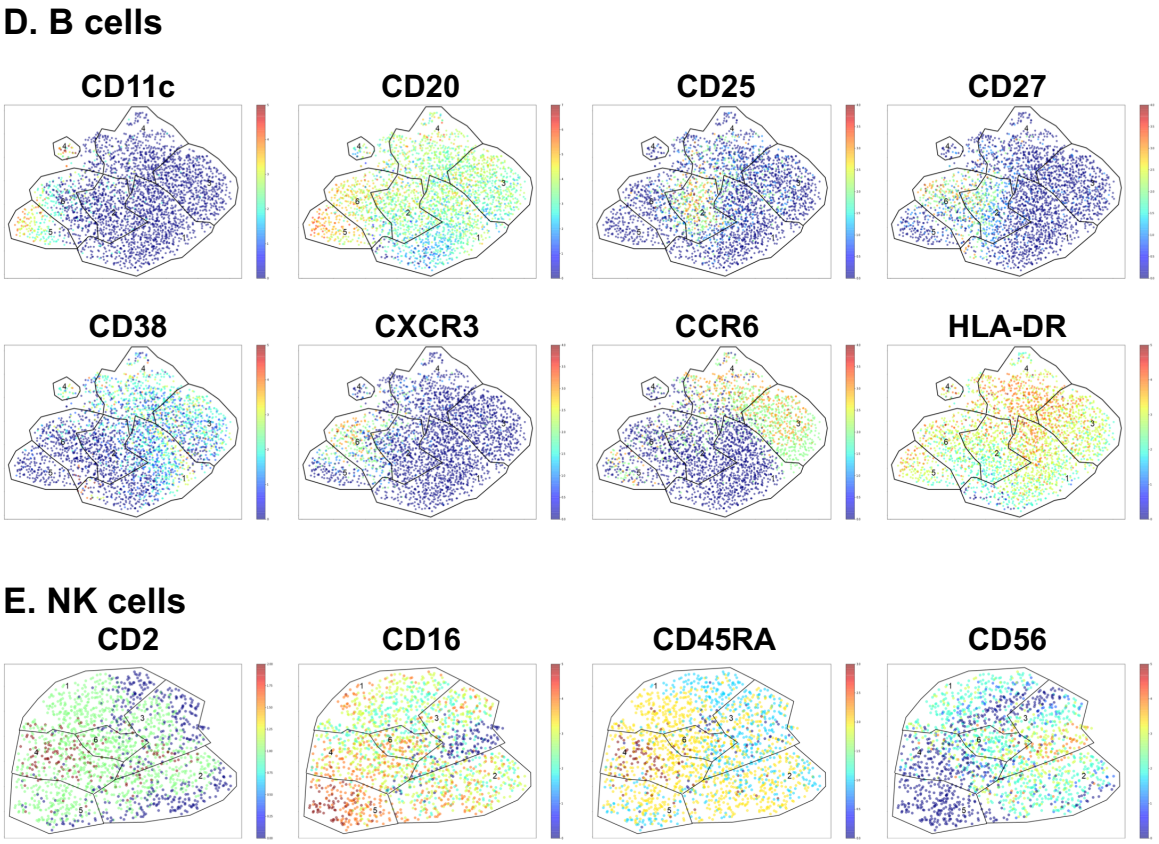

Figure 2

Figure 2. Cell surface marker expression. The expression level of each of the 40 antibody markers was color-coded from dark blue (=0, not expressed) to red (highest expression, log2 scale, as per color bar in each panel). Rainbow plots projected on UMAP gates of each cell type. Selected surface markers shown on top of each plot; all others in Figure S3. Cluster outlines as defined in figure 2. **(A) CD4 T cells**; **(B) CD8 T cells**; **(C) Classical (CM), intermediate (INT) and non-classical (NCM) monocytes; (D) B cells** and **(E) NK cells**. Violin plots of surface marker distribution of each cluster in figure S5. Cluster calling in figure 3.

B cells. As expected, CD20 and CD74 (HLA-DR) were expressed in all B cells. (**Figure 2D**). CD27, IgM and IgD are used to identify naïve B cells (CD27-IgM+IgD+).[27,89] Clusters 1, 3 and 4 were negative for CD27 with high transcript expression for IgM and IgD, consistent with naïve B cells. Clusters 3 and 4 expressed CCR6, a subset found in HIV+ subjects[30]. B cell cluster 2 expressed CD25, which is a known marker for activation for B cell proliferation and exhaustion,[90,91] and CD27, identifying cluster 2 as a likely activated memory B cell. Cluster 5 had high CD11c levels, known to increase in HIV-infected patients,[32] and expressed some CXCR3 and CCR6, but

was CD27^{low}. These features together with moderate expression of CD22 transcript suggest that cluster 5 may contain CD11c+ pathologic B cells.[32] (**Figure 3D**).

NK cells. Most NK cells were mature (CD56^{dim}/CD16+), as expected. Cluster 3 also contained immature (CD56^{bright}CD16-) NK cells. The CD56^{low}CD16- cells (clusters 4 and 5) expressed CD2 and CD45RA. Cluster 5 was CD56-CD16^{high}, an NK cell subset known to be elevated in chronic HIV infection.[69,70] (**Figure 2E, S4, Figure 3E**).

A. CD4 T cells

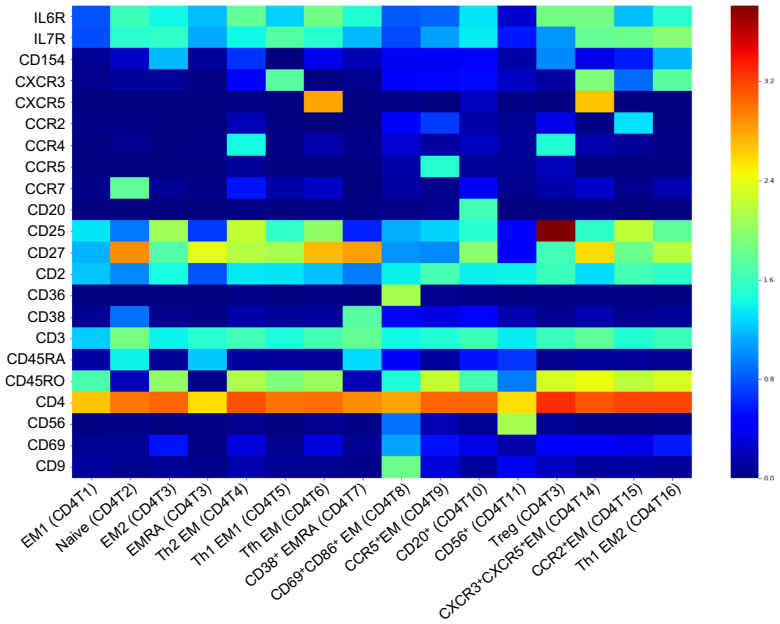

B. CD8 T cells

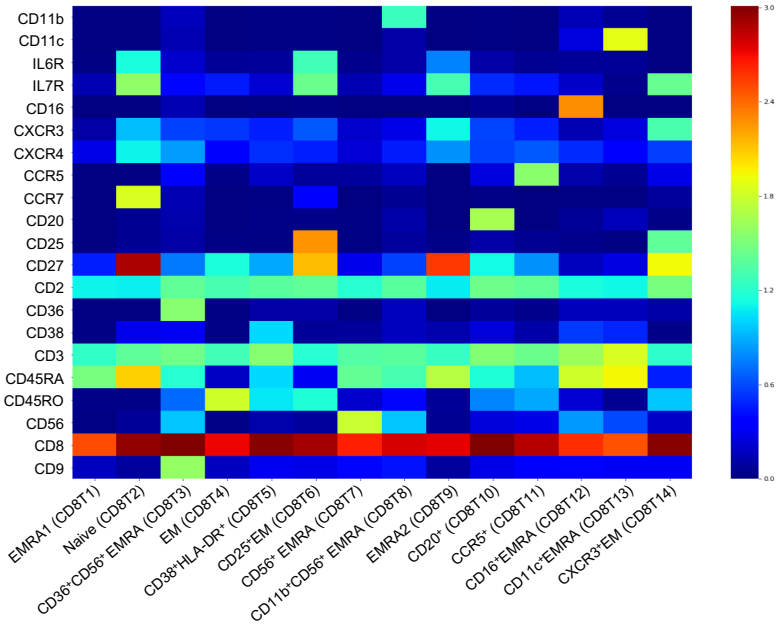

Figure 3

1

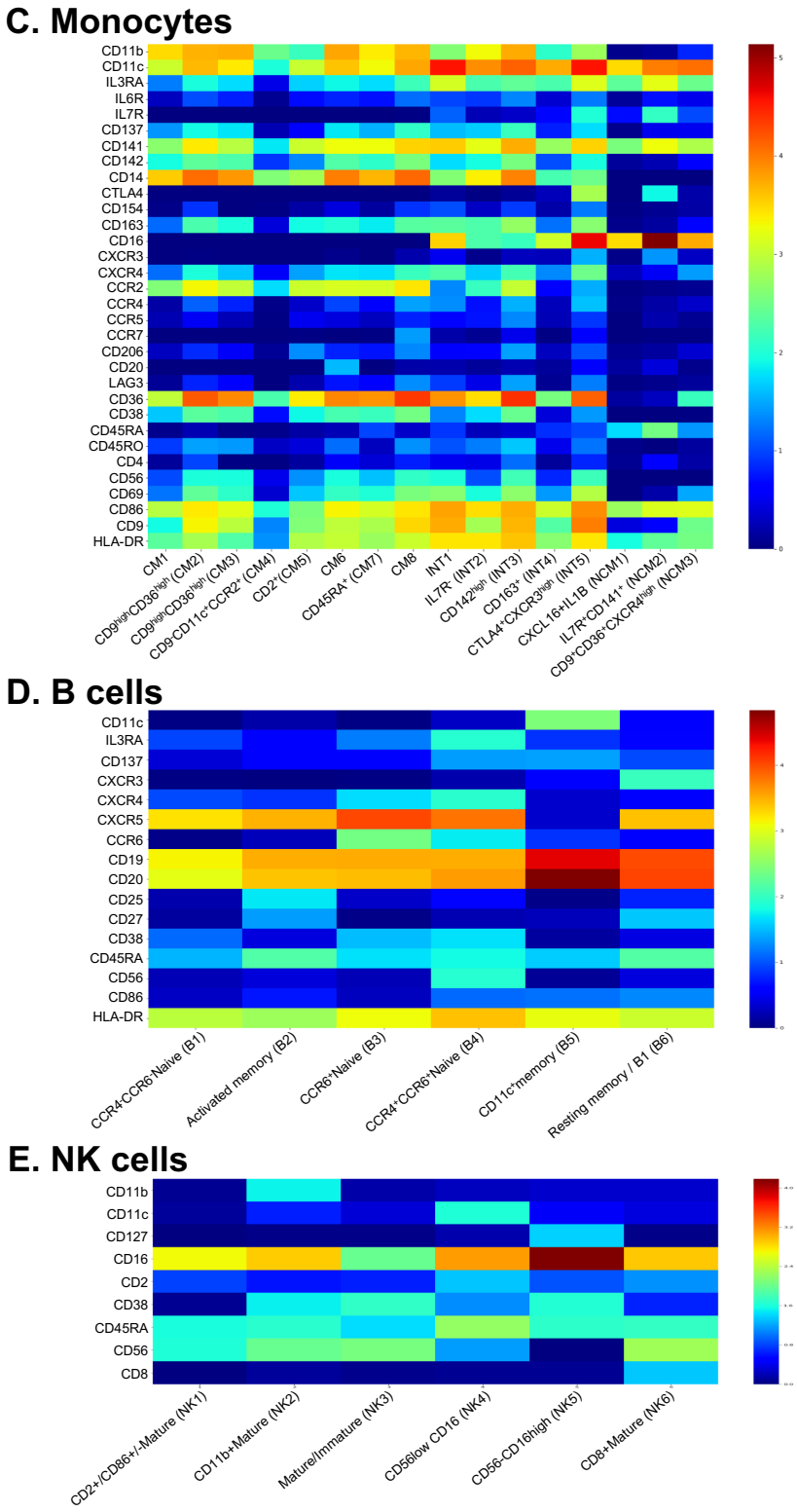

Figure 3

Figure 3. Heatmaps of antibody expression (log2 scale) in each main cell type: A) CD4 T cell, B) CD8 T cell, C) Monocytes, D) B cell and E) NK cells. Immunophenotypes at the bottom. Blank means uncalled. Abbreviations: EM; effector memory, EMRA; terminally differentiated effector memory; CM, Classical Monocyte; INT, Intermediate Monocyte; NCM, Nonclassical Monocyte.

Transcriptomes.

Next, we analyzed the transcriptomes of each single cell (**Excel Table S1**). We tested gene expression of each cluster against all other clusters in each major cell type (**Figure 4**), using Seurat to report the data as log2 fold-change (logFC) and percent of cells expressing each gene. Significant overexpression of *GNLY*, *GZMA*, *GZMH*, *NKG7* and *FGFBP2* together with the surface phenotype (**Figure 3A**) confirmed **CD4 T cell** cluster 1 as effector memory (EM). We found two clusters of EMRA cells that expressed CD25RA with quite different transcriptomes: cluster 8 EMRA overexpressed *CHI3L2* and cluster 9 EMRA cells overexpressed *GNLY*, *GZMA*, *GZMB*, *GZMH*, *NKG7*, *FGFBP2*, *PRF1*, *HOPX*, *FCN1*, the chemokine *CCL3*, the Th1 cytokine *IFNG* and the Th1 transcription factor *TBX21* (**Figure 4A**).

Among CD8 T cells (**Figure 4B**), CD45RA+ cluster 2 was naive based on significant overexpression of *CCR7*, *SELL* and *IL7R*. Cluster 7 was confirmed to contain CD56+ EMRA (NK-like EMRA) based on significant overexpression of *KLRF1*. Cluster 8 (CD11b+CD56+EMRA) significantly overexpressed *S100A9* and *FCN1*. Clusters 12 and 13 had NK-like phenotypes, based on significant overexpression of *FCGR3A*, *GZMB* and *KLRB1*.

In monocytes, CM5 overexpressed *CD1C*, *CLEC10A* and *FCER1A*. Among intermediate monocytes, cluster 3 significantly overexpressed *S100A12*, *CD14*, *CD163*, *CLEC4E*, *THBS1*, *MGST1*, *RNASE2* and *6*. Nonclassical monocytes, B and NK cells showed little differential gene expression. Exact p-values of differential gene expression in all major cell types are in **Table S9**.

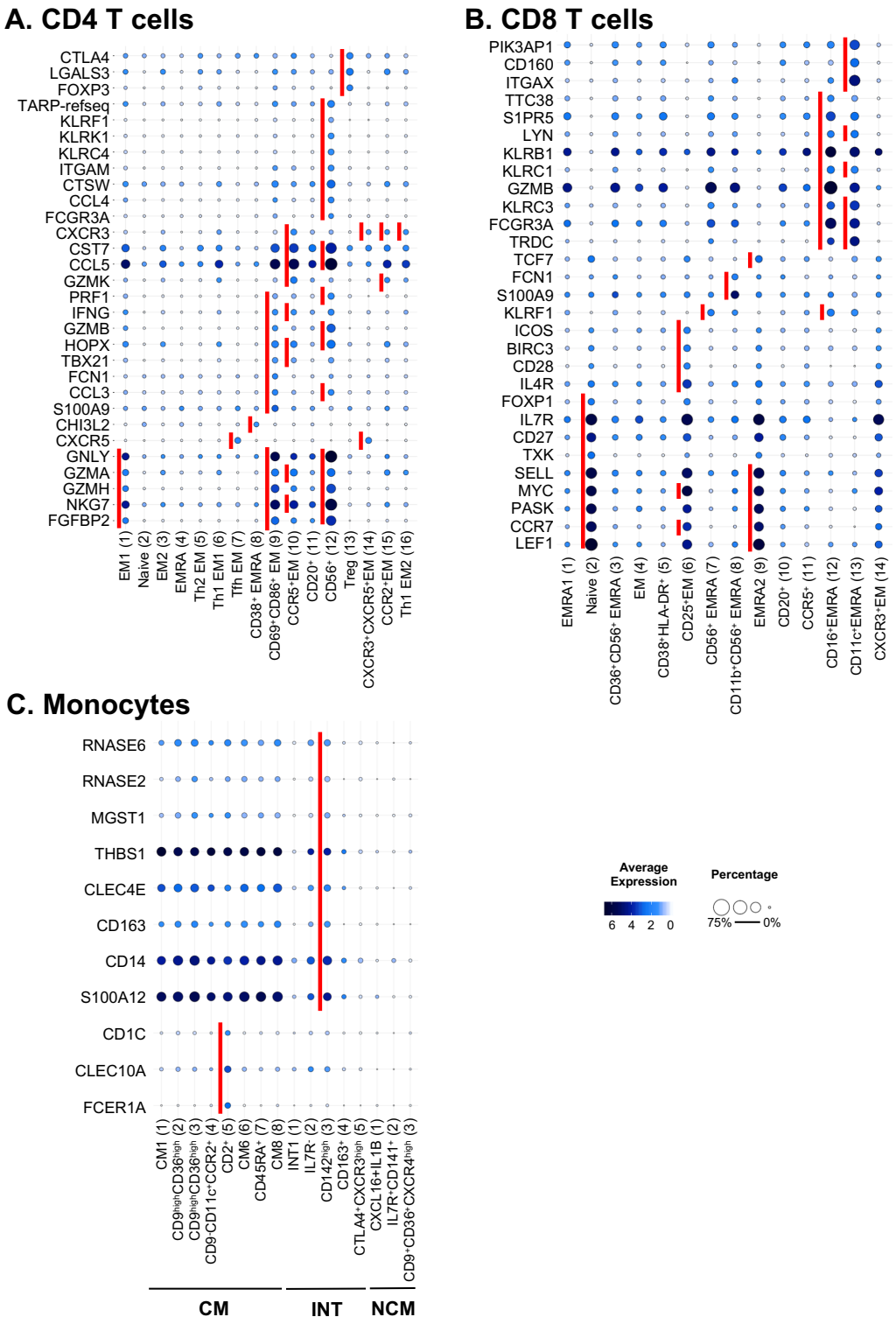

Figure 4

Figure 4. Significantly differentially expressed genes of cells in each cluster. Expression of 485 transcripts was determined by targeted amplification (BD Rhapsody system). Significant genes defined as adjusted p<0.05 and log2 fold change >1. Dot plot: fraction of cells in cluster expressing each gene shown by size of circle and level of expression shown from white (=0) to dark blue (=max, log2 scale). Red bars indicate genes that were significantly higher in each

cluster compared to all other clusters of the parent cell type. **(A) CD4 T cells, (B) CD8 T cells and (C) monocytes** (Classical monocytes; CM, Intermediate monocytes; INT, Non-classical monocytes; NCM)**.**

Ingenuity Pathway Analysis.

To identify pathways enriched in the different PBMC clusters, we used Ingenuity pathway analysis[92]. (**Figure S6, Table 1**) The pathway "communication between innate and adaptive immune cells" was very highly enriched in B cells and several monocyte subsets, with p values below 10^{-10}. The main genes contributing to this enrichment were the chemokines *CCL5* and *CCL8*, the co-activators *CD83* and *CD86*, the Fcε receptor *FCER1G*, major histocompatibility complex-II (*HLA-DRA*), the cytokines interferon-γ (*IFNG*), IL-15 (*IL15*), and IL-1β (*IL1B*), the Toll-like receptors *TLR2* and *TLR8* and the TNF superfamily members *TNF* and APRIL (*TNFSF13*). Th1 and Th2 pathways were highly enriched in several T cell subsets. This enrichment was driven by the TCR signaling subunits *CD3D* and *CD3E*, the co-receptor *CD4*, the co-activator *CD86*, the chemokine receptor *CXCR4*, the adhesion molecule *ICAM1*, interferon-γ (*IFNG*) and its receptor (*IFNGR1*), the IL-2 receptor subunit *IL2RB*, β2 integrins (*ITGB2*), the killer lectin receptor *KLRC1* and *KLRD1* and the transcription factors *RUNX3*, *STAT4* and *TBX21*. The atherosclerosis signaling pathway was enriched in the monocyte clusters INT3, INT5 and CM1. The genes driving this enrichment were the scavenger receptor CD36, lysozyme (*LYZ*), the adhesion molecules PSGL-1 (*SELPLG*), ICAM-1 and integrins α4 (*ITGA4*) and β2 (*ITGB2*), TNF, the known CVD-causative cytokine IL-1β (*IL1B*), the chemokine IL-8 (*CXCL8*), the chemokine receptor CXCR4 and the pro-atherogenic cytokine interferon-γ (*IFNG*). More significantly enriched pathways are shown in **Table 1**.

1 **Table 1. Significantly enriched pathways.**

Antigen Presentation Pathway	**CD8T5, CM5, CD4T13, INT4, CD8T14, CM1, CD8T3, INT3, CD8T2, CD4T9, CM3, CD8T9, CD8T6, CD4T10**, CD4T12, B2, CD4T4, CD8T7, CD4T2, CD8T10, B1, CD4T7, CD8T11
Atherosclerosis Signaling	**INT5, CM1, INT3**, CD4T9, CD4T6, CD8T14, CD4T12, CD8T6, B5, CM5, CD8T2, CD8T7, CM3, B3, INT4, CD8T9, B6, CM7, CD4T8, INT2, CD8T12
B Cell Development	**B2, CD4T13, CD8T5, B1, INT4, CD8T3, B6, INT3, CM5**, CD8T2, B3, B4, CD8T14, CM1, INT5, CM2, CD4T9, CD4T12, CD8T9, CD8T6, CD4T6, CD8T10, INT1, CM3, CM4, CD8T13 CD4T10
Chemokine Signaling	CD8T5, CD8T2, CD4T14, CD4T12, CD8T9, CD8T6, CD8T14, CD8T1, CM5, CD4T1, CD4T8, CD4T9, CD8T7, CD4T2, CD4T6
Communication between Innate and Adaptive Immune Cells	**B4, B6, B2, CD8T6, B3, B5, B1, CD4T12, CD8T9, CM5, CD4T9, CD8T2, INT5, CD8T5, CM1, CD8T13, CM3, CD8T7**, CD4T13, CD8T14, CD8T3, CD4T10, CD8T1, INT3, CD4T4 CD4T1, CD4T8, CD4T2, CM2, CD8T12, CD4T14, INT1
Crosstalk between Dendritic Cells and Natural Killer Cells	**CD4T12, CD8T2, CD8T6, CD8T14, CD8T13, B6, CD8T9, B4, CD4T9, CD4T13, CD8T7, CD8T12, B5, CD4T2**, CD8T3, CD8T1, CD8T5, CD4T4, CD4T8, B3, CM2, B2, CM1, CD4T10, INT3, CD4T1, CD4T16
Cytotoxic T Lymphocyte-mediated Apoptosis of Target Cells	**CD8T12, CD4T12, CD8T2, CD8T7**, CD8T9, CD8T11, B2, CD4T13, CD8T14, CD8T3, CD8T1, CD4T9, CD8T6, CD4T16, CD8T8, B1, CD4T5
Dendritic Cell Maturation	**B6, B5, CM5, B4, INT3, B2, CD4T13**, CM1, B1, CD4T12, B3, INT4, INT5, CD8T5, CD8T6 CD4T4, CD4T15, CD4T8, CM3, CM2, CD8T2, CD4T2, CD8T14, CD8T9, CD8T3, CD8T1
Fcγ Receptor-mediated Phagocytosis in Macrophages and Monocytes	INT5, CD8T12, CM4, CD8T13, CD8T2, CD8T1, INT3, B5, CD8T7, INT2, CD4T12, CD8T9, INT1
Granulocyte Adhesion and Diapedesis	**CM3, CM5, CD4T12, INT5, INT3, CD8T6, CD8T2, CD8T9, CD4T9, CD8T7, CM1**, CD8T12 CD8T5, CD4T8, CD4T6, CD8T14, CD8T13, CD8T3, CD4T14, CD8T1, CD4T4, B5, CD4T1 CD8T4, CD4T2, CD8T11, CD4T13, INT4, CM4, CD4T10, CM7
IL-7 Signaling Pathway	**B5, CD8T2, CD8T5**, CD8T14, CD8T13, CD4T10, CD8T10, CD4T9, CD8T7, CD8T12, B1 CD4T12, B3, CD8T11, CD8T9, CD8T6, B2, CD8T3, B6, CD8T1, CD4T4, CD4T1, CD4T2 CD4T6, CD4T14, CD4T3
Interferon Signaling	B3, B5, CD8T2, INT1, CM3, B4, CM4
Natural Killer Cell Signaling	**CD8T12, CD8T13, CD8T2, INT5, CD4T12**, CD8T7, CD4T2, CD8T14, CD4T10, CD8T9, CD8T6, CD4T8,

	CD8T3, CD8T1, CD4T4, CD8T11, B2, CD4T13, CD8T5
Necroptosis Signaling Pathway	CD4T5, CD4T2, CM5, CD4T1
Phagosome Formation	**B5, CM5, B6, INT5, B1,** B2, CM4, CD8T12, B3, B4, CD4T12, CD8T14, CD8T13, INT3 CD4T6, CD8T7, INT2
T Cell Receptor Signaling	**CD8T2, CD8T12**, CD4T8, CD4T2, CD8T11, CD4T12, CD8T6, CD4T4, CD4T1, CD8T7
Th1 and Th2 Activation Pathway	**CD8T2, CD4T12, CD8T6, CD8T9, CD8T12, CD8T14, CD4T10, CD4T9, CD8T5, B2, CD4T8, CD4T2, CD8T13, CD8T3, B6, CD4T7, B5, CD4T13, CM5, CD4T1, CD8T7**, CM1, CD4T15, CD4T4, B3, INT4, CD4T16, CD4T14, CD4T3, INT3, B1, CM3, CM2, B4, CD8T11, INT5, CD8T1, CD4T6
Th1 Pathway	**CD8T2, CD4T12, CD8T6, CD8T9, CD4T10, CD8T12, CD4T9, CD8T14, CD8T3, CD8T5** **CD4T7, CM1, CD8T13, CD4T15**, CM5, CD8T7, B2, CD4T13, INT4, CD4T16, B6, INT3 B5, CD4T1, CD4T8, CD4T2, CM3, CM2, B4, CD8T11, INT5, CD8T1, CD4T4
Th17 Activation Pathway	CM1, INT5, CD4T12
Th2 Pathway	**CD8T2, CD4T12, CD8T9, CD8T6, CD8T14, CD4T10, CD8T12, CD8T5, B2, CD4T8, CD4T9, CD4T2, CM5, CD4T1, CD4T13, CD8T3, B6**, CD4T4, B5, CD4T7, CD8T7, INT4, CM1, INT3, CD4T3, B1, CD4T15, CM3, CM2, B3, CD8T13, CD4T6
Toll-like Receptor Signaling	**CM5**, CM3, INT5, INT3, CD4T1, CD4T2, INT1
TREM1 Signaling	**CM5, CM1, CM3**, CM4, INT5, B6, B5, B4, CM2, CD8T13, INT3, CD4T9, CM7, CD4T12, CD4T3, CD8T2

All pathways shown were significantly enriched in the clusters indicated. **Bold: P<0.0001,** others p<0.05**.**

Gene expression changes by HIV, CVD and cholesterol control.

Next, we reasoned that HIV, CVD and cholesterol control would be associated with specific gene expression changes. We focused non-HIV vs HIV+ (reflecting the HIV signature), HIV+ vs HIV+CVD+ (reflecting the CVD signature), and HIV+CVD+ vs HIV+CVD+ treated with LDL cholesterol-lowering drugs (reflecting the cholesterol control signature) (**Figure 5**). In a bulk RNA-Seq study, we found that statins had a strong effect on sorted classical monocyte transcriptomes.[15] In 27 of the 58 PBMC clusters, expression of hundreds of genes was significantly (adjusted p<0.05) regulated; 181 between women with and without HIV, 465 between

women with HIV and women with HIV and CVD, and 303 in women with HIV and CVD that received cholesterol-lowering drugs. We discovered by far the most regulated genes in classical monocytes: 98 in cluster 1, 88 in cluster 2 and 55 in cluster 3. The top 10 highly regulated genes for the main cell types are shown in **Table S10** and all the underlying gene expression data in **Excel table S2**. **Figure 5** shows the cell types with the most regulated genes; volcano plots for clusters with fewer genes are shown in **Figure S7**.

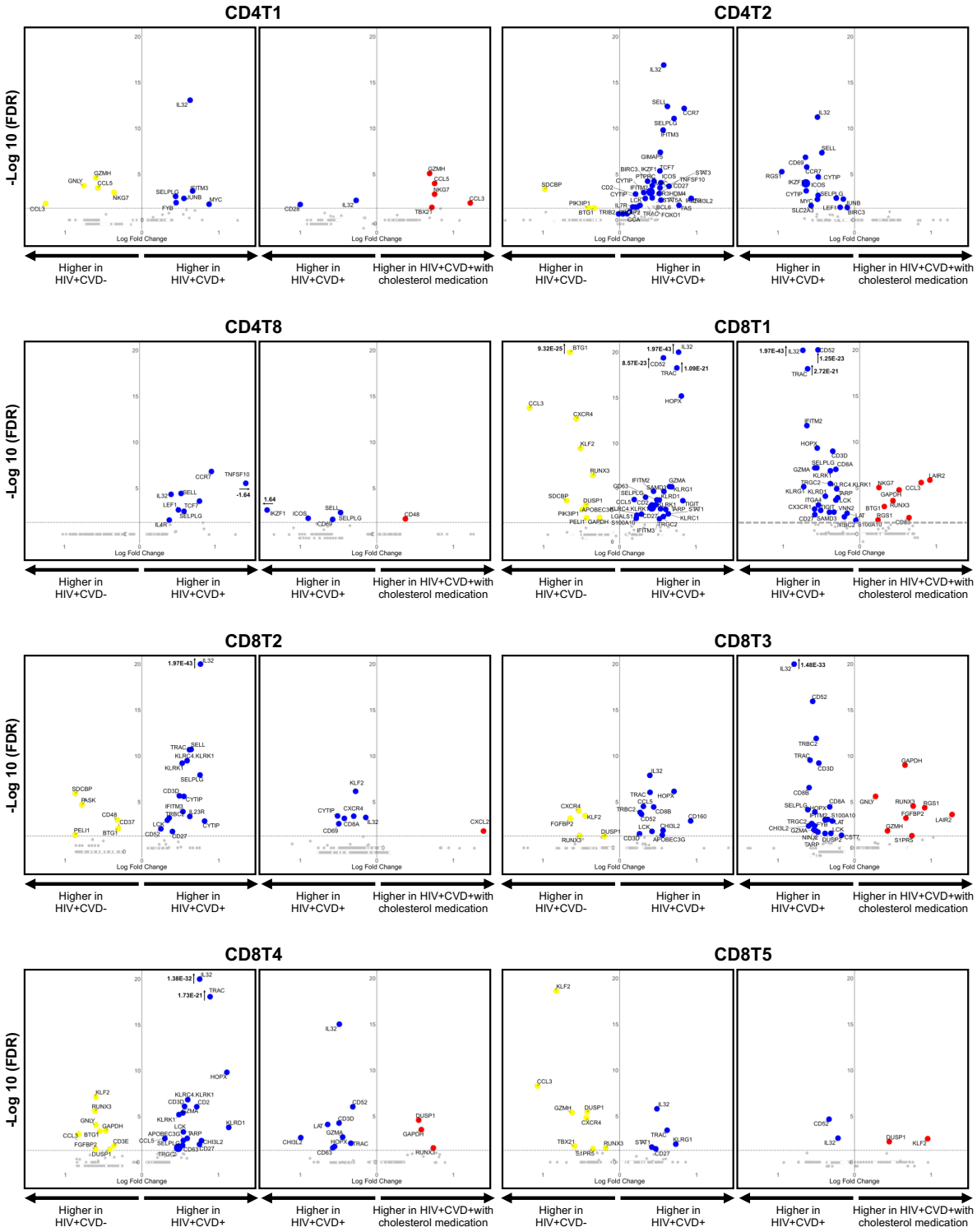
CD4T1
CD4T2
CD4T8
CD8T1
CD8T2
CD8T3
CD8T4
CD8T5
-Log 10 (FDR)
Log Fold Change
Higher in HIV+CVD-
Higher in HIV+CVD+
Higher in HIV+CVD+
Higher in HIV+CVD+with cholesterol medication

Figure 5

1

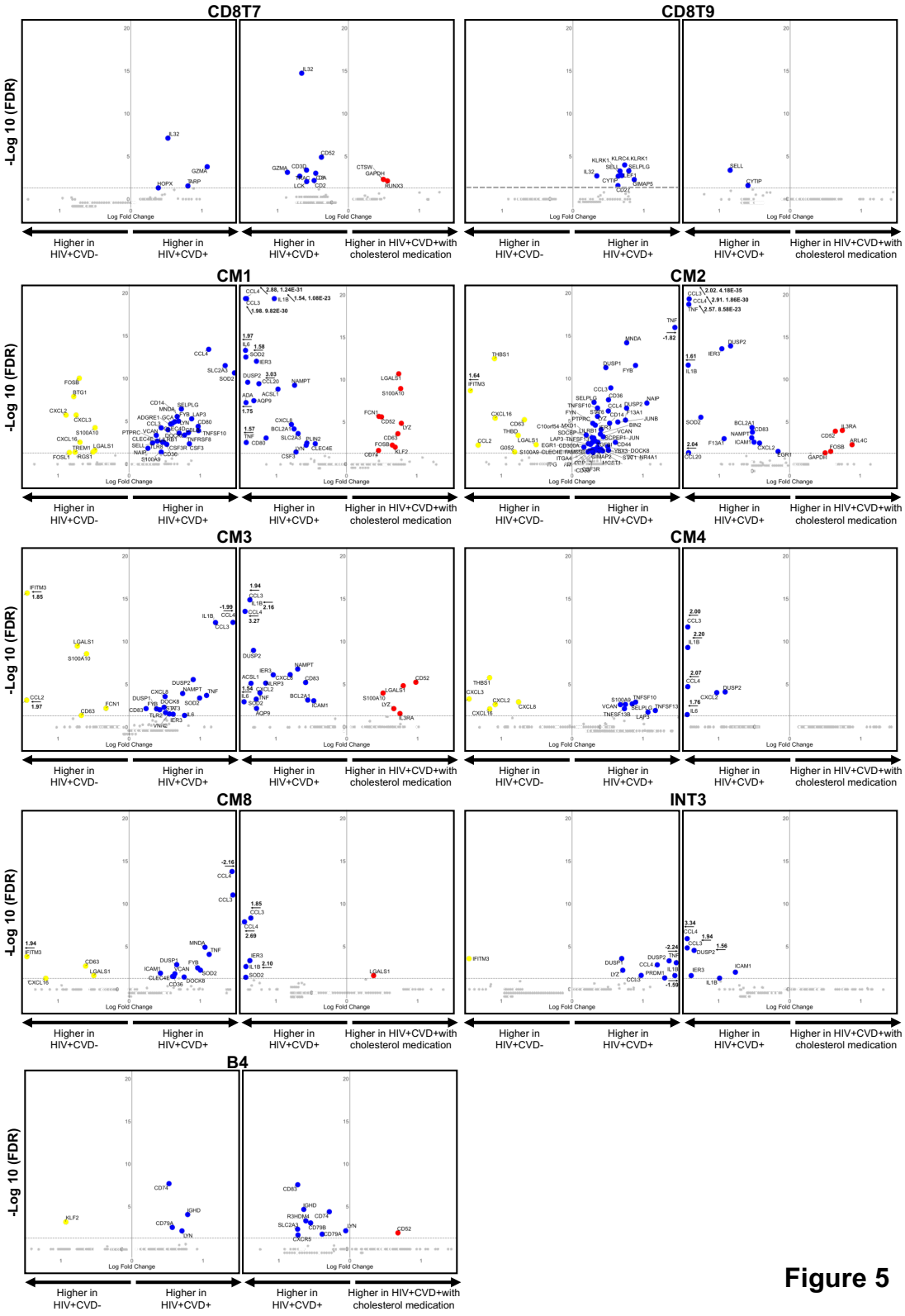

Figure 5

Figure 5. Volcano plots comparing gene expression in single cells from WIHS participant types in each cluster. All 3 meaningful comparisons were calculated, but this figure is focused on HIV+CVD- vs HIV+CVD+, and HIV+CVD+ vs HIV+CVD+ with cholesterol medication; all clusters in which at least 10 genes were statistically significant. Colored

dots (HIV+CVD- yellow, HIV+CVD+ blue, and HIV+CVD+ with cholesterol medication red) indicate significantly differentiated expressed genes (FDR<0.05 and |log2FC|>2). 3 CD4 T and 7 CD8 T cell clusters, 5 CM and 1 each INT and B cell clusters met these criteria. Dashed line indicates adjusted p-value of 0.05. Additional volcano plots shown in Figure S7, full data set shown in Excel Table S2.

T cells. In CD4T1, 2 and 8, IL-32 was highly significantly increased by CVD, which was reversed by cholesterol lowering in CD4T1 and 2 (**Figure 5, Table S11**). IL-32 is an inflammatory cytokine that is known to be important in CVD.[93–95] In CD4T2, L-selectin (*SELL*), PSGL-1 (*SELPLG*) and *CCR7* were also highly significantly increased in WIHS participants with HIV and CVD, and significantly corrected by cholesterol lowering (**Figure 5**). In addition to *SELL* and *SELPLG*, CD4T8 showed strong upregulation of TNFSF10 (*TRAIL*). In CD8T1 and 2, *IL32* was strongly induced in women with CVD and significantly corrected by cholesterol control. Other genes highly induced by CVD in CD8T1 included *CD52*, *TRAC* and *HOPX*. Several killer cell lectin receptors (*KLRC4*, *KLRD1*, *KLRG1*, *KLRK1*) were also significantly upregulated in CVD and restored to near-control by cholesterol-lowering drugs. In CD8T2, the activation marker CD69 was significantly downregulated by cholesterol-controlling drugs. In CD8T3, *CD52, CCL5, IL32* and *CD160* were all significantly upregulated by CVD. *CCL5* encodes the chemokine RANTES, known to be important in atherosclerosis.[96] In CD8T4, CVD significantly increased *IL32, TRAC, HOPX, CCL5* and the killer lectin receptors *KLRK1, KLRC4, KLRD1* (figure 5).

In classical monocyte cluster 1, CVD strongly and significantly increased *CCL4, SLC2A3, SOD2* and *SELPLG,* all reversed by cholesterol control. In CM2, *TNF, DUSP1 and 2* were highly upregulated by CVD (**Figure 5**), as were TNFSF10 (*TRAIL*), TNFSF13 (*APRIL*) and TNFSF13B (*BAFF*). *BAFF* and *APRIL* are important B cell regulators.[97,98] In addition to *CCL3*, *CCL4* and *DUSP2*, *IL1B,* known to be highly relevant in atherosclerosis,[99] was highly upregulated in CM3 of HIV+CVD+ participants. The Toll-like receptor TLR2, which is known to be involved in atherosclerosis,[100–102] was upregulated by CVD in CM3. In **intermediate monocyte** cluster 3,

CCL3, *CCL4, TNF, IL1B* and *DUSP2* were upregulated by CVD and most were corrected by statin treatment.

Gene expression patterns in WIHS participants with HIV and CVD.

Figure 5 showed that many genes were significantly upregulated by HIV and CVD and corrected by cholesterol control. We systematically explored such patterns of gene expression (**Figure 6**). The most common pattern, seen in 21 genes, was decreased expression in women with HIV, increased in CVD and corrected by cholesterol control (down-up-down). Twelve other genes showed increased expression in participants with HIV, further increased in participants that also had subclinical CVD, and then reduced in participants on cholesterol-lowering drugs (up-up-down). We found 3 genes that were significantly upregulated in participants with HIV, reduced in participants with CVD, and further reduced by cholesterol control (up-down-down). One gene, interferon-γ receptor (IFNGR1) was reduced by HIV, even more reduced in presence of CVD, and further reduced cholesterol-lowering drug treatment (down-down-flat, **Figure 6**).

T**he down-up-down pattern** was the most common in CD4 T cells (**Figure 6A**). The chemokine receptor *CCR7* and the adhesion molecules L-selectin (*SELL*) and PSGL-1 (*SELPG*), the inflammatory cytokine IL-32 (*IL32*) and the cytoskeleton modulator *CYTIP* all followed this pattern. In CD8 T cells (**Figure 6B**), *IL32, SELPLG*, the killer lectin receptors *KLRD1*, *KLRG1*, *KLRK1* and the interferon-responsive gene *IFITM2* all followed this pattern. In classical (**Figure 6C**) and intermediate monocytes (**Figure 6D**), TNF showed the down-up-down behavior, as did *IL1B* in intermediate monocytes. In non-classical monocytes, *CCL4* and *CD52* were downregulated in participants with HIV, up in participants with CVD and corrected by cholesterol control (**Figure 6E**). In B cells, *CD74* and the BCR subunits *CD79A* and *CD79B* were down by HIV, up by CVD and corrected by cholesterol-lowering drugs (**Figure 6F**). Finally, this pattern was also seen for two Fc receptor genes in NK cells, *FCGR3A* and *FCER1G* (**Figure 6G**).

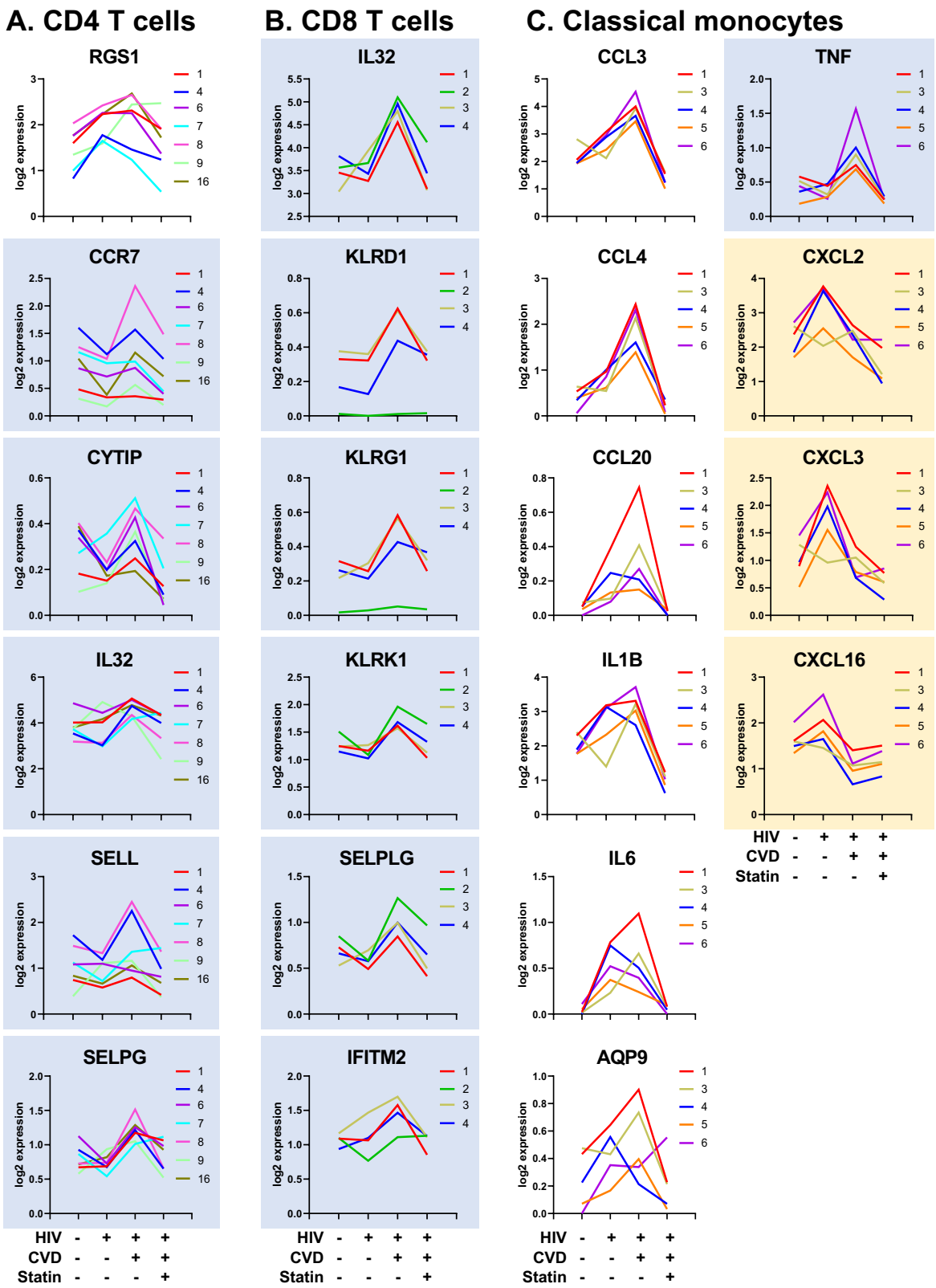
A. CD4 T cells
B. CD8 T cells
C. Classical monocytes
RGS1
IL32
CCL3
TNF
CCR7
KLRD1
CCL4
CXCL2
CYTIP
KLRG1
CCL20
CXCL3
IL32
KLRK1
IL1B
CXCL16
SELL
SELPLG
IL6
SELPG
IFITM2
AQP9
log2 expression
HIV - + + +
CVD - - + +
Statin - - - +

Figure 6

1

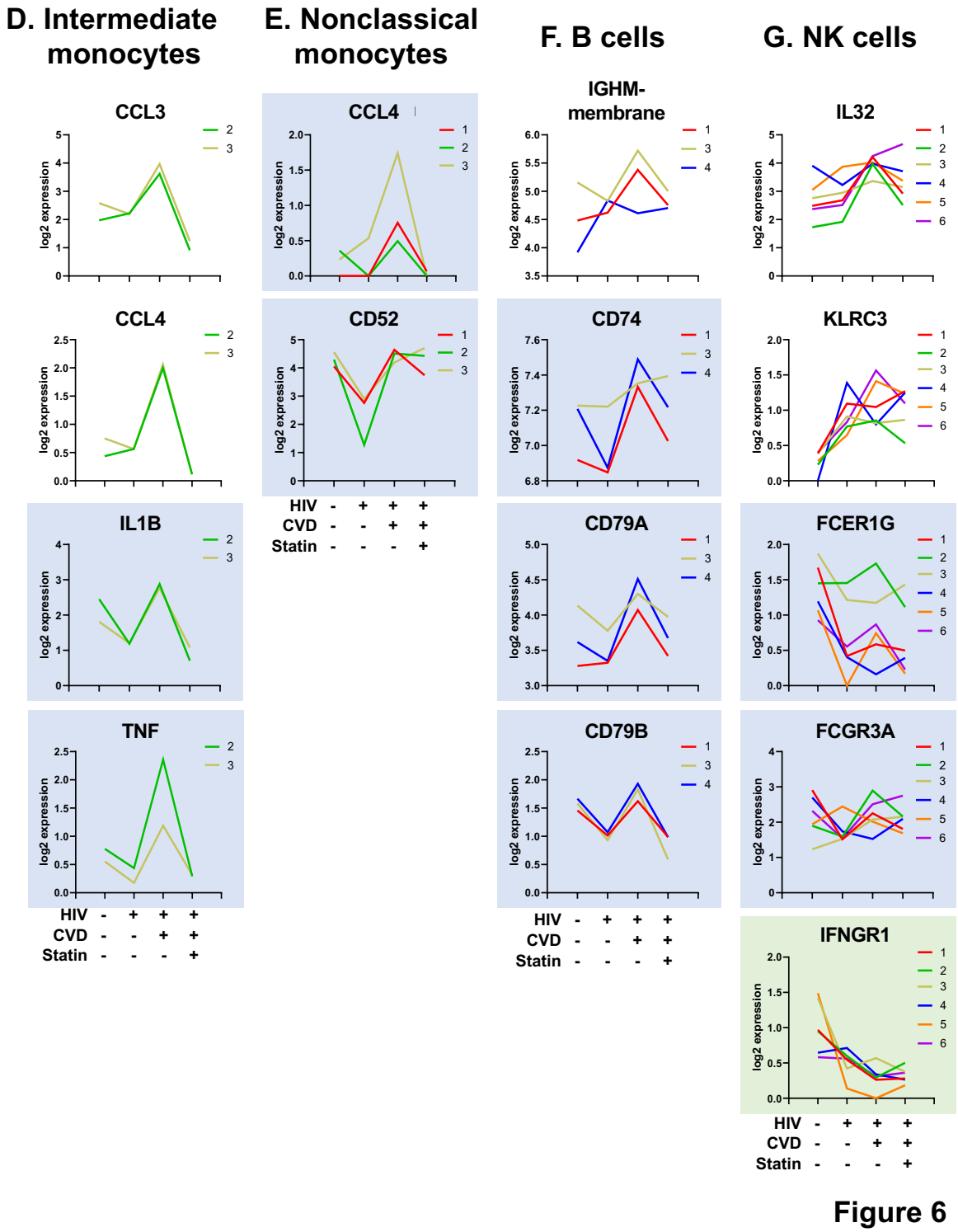

Figure 6. Gene expression patterns by HIV, CVD and cholesterol medication. The log2 normalized expression of the genes listed above each panel shown as line graphs for each of the indicated cell types (average of all cells). Genes selected by significant differential expression. All data shown as HIV-CVD-, HIV+CVD-, HIV+CVD+, HIV+CVD+ on cholesterol medication (statin), from left to right. The line graph patterns were categorized as up-up-down (white

background), down-up-down (blue background), up-down-down (yellow background), and down-down-flat (green background).

The up-up-down pattern was the most common in classical monocytes (**Figure 6C**), where the inflammatory chemokines CCL3, CCL4 and CCL20, the inflammatory cytokines IL1B and IL6, and the water channel AQP9 followed this pattern. In intermediate monocytes, *CCL3* and *CCL4* also followed this pattern, as did membrane-bound IgM (*IGHM*) in B cells (**Figure 6F**). *IL32* and *KLRC3* in NK cells were upregulated in women with HIV, further increased by CVD and downregulated by cholesterol-lowering drugs (**Figure 6G**).

The up-down-down pattern was less common. It was characteristic of CXCL chemokines in classical monocytes (**Figure 6C**), specifically the neutrophil-attracting chemokines CXCL2 and CXCL3 as well as the CXCR6 ligand CXCL16, which is also a scavenger receptor.[103–105] The underlying raw data for figure 6 is presented as **Excel Table S3**.

PBMC subsets with significant differences of abundance.

Finally, we asked whether HIV and CVD affected the abundance (cell number) of PBMC subsets. As expected,[46,106] we found that CD4 T cells were significantly reduced in people living with HIV. We compared the proportions (cell percentages) for each of the 58 clusters using log odds ratio followed by ANOVA and Tukey's multiple comparison test. We compared non-HIV vs HIV+ (reflecting the HIV effect), HIV+ vs HIV+CVD+ (reflecting the CVD effect), and HIV+CVD+ vs HIV+CVD+ treated with LDL cholesterol-lowering drugs (reflecting the cholesterol control effect) (**Figure 7**). Strikingly, three subsets of **intermediate monocytes** (**Figure 7A**) showed significantly different proportions. INT2 (IL7R-) and INT3 (TF^{hi}) were significantly elevated in WIHS participants living with HIV and then drastically reduced in those that also had subclinical CVD. Cholesterol control significantly restored these cells. INT4 had an opposite pattern: These CD163- cells disappeared in WIHS participants living with HIV, reappeared in those that also had subclinical CVD, and were slightly reduced by cholesterol control.

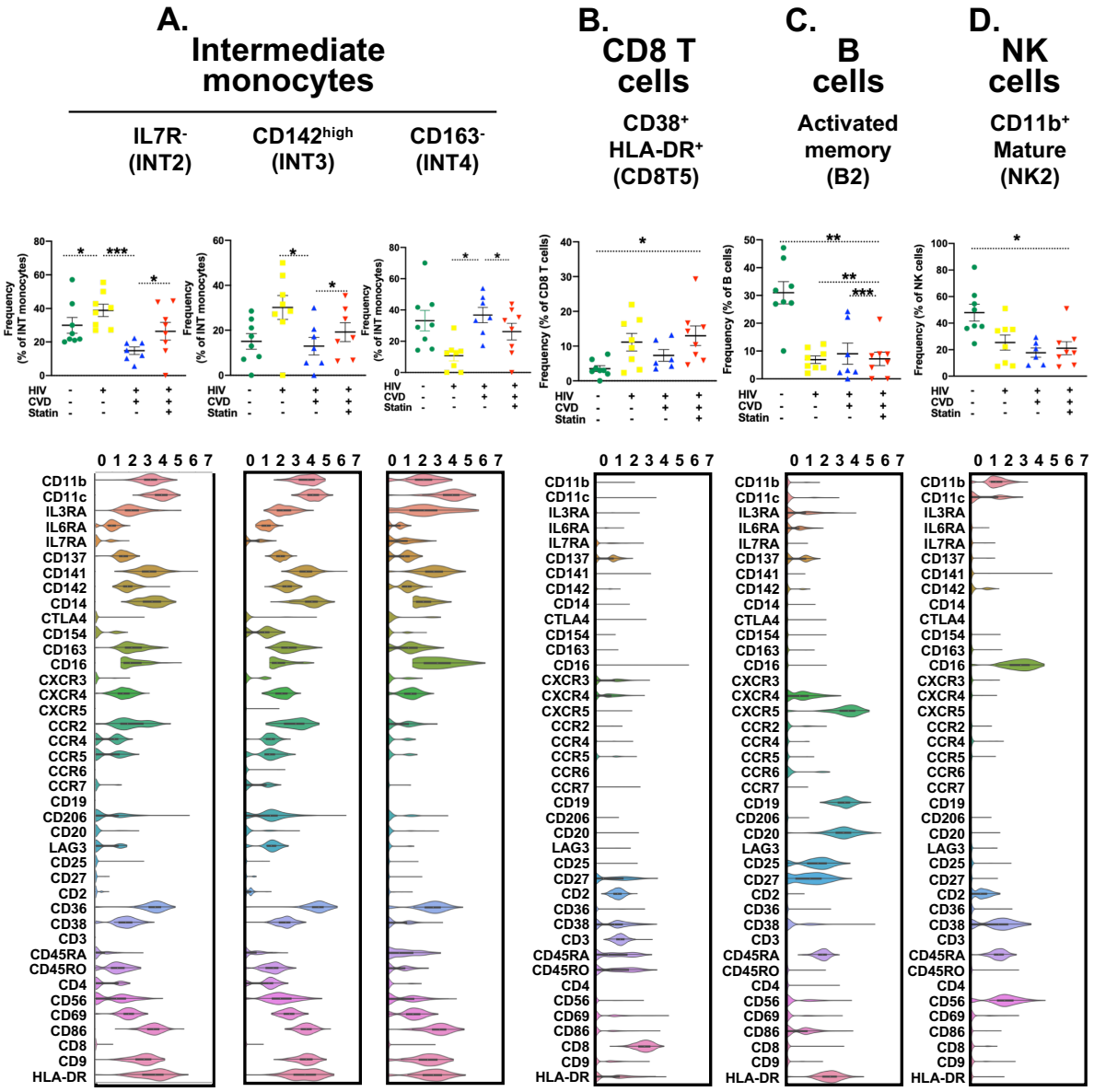

Figure 7

Figure 7. Cell proportions in women with HIV, CVD, both or neither. HIV-CVD- (green), HIV+CVD- (yellow), HIV+CVD+ (blue), HIV+CVD+ on cholesterol medication (statin, red), from left to right. 8 samples per group except 7 for HIV+CVD+. Proportions of cells in each cluster calculated as percent of the parent cell type as indicated in the title of each panel. Clusters with significant differences (*, p<0.05, **, P<0.01, *** p<0.001) in cell proportions (by log odds ratio) are shown with individual data points representing the standard error of the mean (SEM). Violin plots below show expression of all 40 cell surface markers (Log2 scale). Cluster description is as in figure 2 and 3.

Among **CD8 T cells,** CD8T5 (CD38+HLA-DR+) (**Figure 7B**) were rare in HIV-CVD- WIHS participants, but increased in disease, becoming significant in HIV+CVD+ treated with cholesterol-

lowering medications. Among **B cells**, activated memory B2 cells (**Figure 7C**) were severely lower in all diseased WIHS participants, whether they lived with HIV or also had subclinical CVD. Among **NK cells,** CD11b+ mature NK cells (cluster 2) (**Figure 7D**) were reduced in women with HIV with or without CVD.

Discussion

Here, we used combined protein and transcript panel scRNA-Seq to identify 58 clusters of PBMCs in 31 participants of the WIHS study. The most diversity was in CD4 T cells (16 clusters), monocytes (16 clusters) and CD8 T cells (14 clusters). B cells and NK cells were resolved into 6 clusters each. The most salient findings were that many inflammatory genes were significantly increased in WIHS participants with CVD, and many of these genes were downregulated in participants on cholesterol-lowering drugs. Six clusters showed significantly different abundance of cells in the four groups of participants, three of them intermediate monocyte subsets, which underscores the extraordinary importance of this cell type in chronic HIV infection[107,108] and CVD[109,110]. Intermediate monocyte numbers have previously been found to be increased in peripheral artery occlusive disease[111] and significantly predicted cardiovascular events.[82,112] Here, we discovered 5 subsets of intermediate monocytes. Intermediate monocyte subsets have not been described before.

INT1, the largest cluster, express the defining intermediate monocytes markers CD14 and CD16. They also share CD11b, CD11c, CD9, CD36, CD38, CD56, CD69, CD83, IL-3RA, IL6R, CD137, CD141, CD142 (tissue factor), CXCR4 and CD74 (HLA-DR) with all other intermediate monocytes. We found no single positive marker that was specific for INT1 and thus refrained from naming this cluster. INT2 uniquely lacks IL-7R (CD127, table 1); we propose to call these cells IL-7R^{-} intermediate monocytes. INT2 cells also lack CXCR3. INT3 (CD142^{hi}) express tissue factor, the initiator of coagulation, even more strongly than INT2. Tissue factor expression has previously been found in intermediate monocytes[110] and was increased in HIV+ subjects[14]. The proportion

of INT2 and INT3 is increased in women living with HIV. Intermediate monocytes are considered pro-atherogenic,[79] and tissue factor expression provides a plausible reason for this. In INT2 and INT3, the inflammatory chemokines CCL3 and CCL4 and the known pro-atherogenic cytokine IL-1β are significantly upregulated in participants with CVD. This is fully reversed in subjects receiving cholesterol-lowering medication. INT4 uniquely lack expression of CD163, the receptor for hemoglobin-haptoglobin complexes. Thus, we call INT4 $CD163^{-}$ intermediate monocytes. INT5, called $CTLA4+CXCR3^{hi}$, uniquely express CTLA4 (CD152) and highly express CXCR3. Since intermediate monocyte subsets are currently not defined in mice, more discovery research in mice is needed to address the function of these intermediate monocyte subsets.

In peripheral blood, we confirmed that CD4 T cells counts were significantly lower in people living with HIV. In many CD4 T cell clusters, *IL32* mRNA expression was prominently increased by CVD. IL-32 is a 27 kDa cytokine expressed in T cells, NK cells and monocytes that is secreted after apoptosis. It is an inflammatory cytokine that drives IL-1β,[99] TNF, IL-6 and IL-8 expression,[94,95] cytokines that are known to be important in CVD. IL-32 activates the leukocyte surface protease PR3, which in turn triggers the G-protein coupled receptor PAR2 and is known to be important in viral infections.[113] We found IL-32 highly expressed in most T and NK cell clusters. IL-32 expression appears to be specific for CVD and responds to cholesterol lowering. Prospective studies in larger cohorts will be needed to determine whether *IL32* mRNA is a useful biomarker.

One of the most striking findings of our study was that many pro-inflammatory cytokines and chemokines that were increased in CVD in many cell types were corrected by treatment with cholesterol-lowering drugs (mostly statins, see **Table S1**). Statins are known to lower several inflammatory biomarkers.[114] Rosuvastatin is known to decrease the progression of subclinical atherosclerosis in HIV+ subjects,[115] which was previously attributed to cholesterol lowering. A large ongoing clinical trial, the Randomized Trial to Prevent Vascular Events in HIV (REPRIEVE), is testing the effects of pitavastatin on CAD and inflammatory biomarkers.[116] Our data suggest

that, in addition to LDL cholesterol lowering, statin treatment has significant anti-inflammatory benefits. This has been shown in earlier studies[117] and our findings greatly extend this to many human blood cell types.

When analyzing gene expression differences among the participant types, we found two common patterns. The up with HIV-up with CVD-down with statin (up-up-down) pattern of gene expression can perhaps be called the expected pattern, since both HIV and CVD are pro-inflammatory, and since statins are known to be anti-inflammatory.[117] However, we also found many genes that followed the down-up-down pattern, which means that their expression was decreased by HIV, increased by CVD and corrected by cholesterol control. Thus, not all inflammatory genes are regulated in the same direction by HIV and CVD, suggesting that for some genes, HIV and CVD are synergistic, for others antagonistic. Consistently across cell types, controlling LDL cholesterol showed an anti-inflammatory gene signature.

In this study, CVD was assessed by carotid ultrasound. Thus, some of the markers discovered here may be expected to be better indicators for stroke than CVD elsewhere. There is overlap between stroke, myocardial infarction and peripheral artery disease risk, but the correlation is not perfect.[118] This discovery study will encourage prospective epidemiological studies to address which PBMC subsets are best suited as clinical biomarkers to stratify risk and guide treatment in subjects with CVD or coronary artery disease or peripheral artery disease.

In the WIHS study, participants were exceptionally well phenotyped, attending semi-annual follow-up visits, during which they underwent detailed examinations, specimen collection, and structured interviews assessing health behaviors, medical history, and medication use.[119] These significant strengths are balanced by limitations of the present study. We don't know whether the same changes in PBMCs would be observed in non-HIV populations. The multiethnic study of atherosclerosis (MESA[120]) is an example of such a cohort. The current findings also need to be extended to men (the current data is based on women) and Caucasians (the current data is based on mostly African American and Hispanic women). Studies of CVD in non-smokers are

also needed (the current data is based on smokers and ex-smokers), and the age range needs to be broadened.

Six PBMC clusters showed significantly changed proportions in response to HIV, CVD, cholesterol control, or combinations. This finding is directly translatable, because these cells are defined by surface markers and thus can, in future validation studies, be identified by standard flow cytometry (**Table S12**), a method that is routinely used in monitoring HIV+ people.[121]

CD8 T cell numbers in HIV+ males are associated with increased risk of acute myocardial infarction.[24] The effect of cholesterol-lowering drugs on CD8 T cell activation is unclear.[25,26] Major clinical trials have shown a potential benefit (reduced CVD risk) in HIV-infected populations treated with statins,[116] but the specific cell types affected were not known prior to the present study. Here, we show that the TEMRA clusters CD8T1, 3, 7 and 9, naïve CD8 T cells (CD8T2), effector memory CD8 T cells (CD8T4) and CD38+ CD8 T cells (CD8T5) all show significant decreases in inflammatory gene expression in subjects treated with cholesterol-lowering drugs.

It is known that HIV disease leads to impaired B cell and antibody responses.[122] Our study identified B cell cluster 2 with high expression of CD25, a known marker for B cell proliferation, activation and exhaustion,[91] suggesting that premature exhaustion of these B cells could be linked to a decreased antibody response in HIV+ individuals.[91] CD11c+ B cells are increased in number in HIV infected patients, which agrees with our observation in B cell cluster 5. A recent study showed that a putative human B-1 cell may be linked to atherosclerosis.[28] Specifically, the percentage of circulating CD20+CD27+CD43+ cells was directly correlated with levels of IgM to oxidation-specific epitopes on low density lipoprotein (LDL) and inversely correlated with coronary artery plaque volume, especially in cells with high expression of CXCR4.[28] Here, we found significantly decreased CXCR4 surface expression in several B cell clusters in subjects with CVD, supporting the idea that CXCR4 on some B cells may have atheroprotective roles. Among NK cells, we found the proportion of cells in cluster 2 to be significantly reduced in HIV+CVD+ participants that were on cholesterol-lowering drugs. $CD56^{bright}$ NK cells are known to accumulate

in human atherosclerotic lesions, possibly contributing to plaque instability.[123] Symptomatic carotid atherosclerotic plaques are often infiltrated by NK cells,[123] but the exact subset was not investigated and their mechanistic role remains unknown.

In conclusion, we present the first study of scRNA-Seq with cell surface phenotype assessment in the same cells in people living with HIV, with and without documented CVD. Beyond the translational and clinical utility of our findings, the identification of 58 distinct clusters of CD4 and CD8 T cells, monocytes, B cells and NK cells helps to gain a deeper understanding of PBMCs, a rich and readily accessible source of biological and clinical information. The discovery of subsets of intermediate monocytes calls for identifying such subsets in model organisms to test their function in vivo. Many inflammatory genes are upregulated by HIV, CVD or both, and in most cases corrected by statin treatment.

Methods

Study characteristics and sample selection. The Women's Interagency HIV Study (WIHS) was initiated in 1994 at six (now expanded to ten) U.S. locations.[36,37] It is an ongoing prospective study of over 4,000 women with or at risk of HIV infection. Recruitment in the WIHS occurred in four phases (1994-1995, 2001-2002, 2010-2012, and 2013-2015) from HIV primary care clinics, hospital-based programs, community outreach and support groups. Briefly, the WIHS involves semi-annual follow-up visits, during which participants undergo similar detailed examinations, specimen collection, and structured interviews assessing health behaviors, medical history, and medication use. All participants provided informed consent, and each site's Institutional Review Board approved the studies.

All participants in the current analysis were part of a vascular substudy nested within the WIHS.[124,125] The baseline visit for the vascular substudy occurred between 2004 and 2006, and a follow-up visit occurred on average seven years later. Participants underwent high-resolution B-mode carotid artery ultrasound to image six locations in the right carotid artery: the near and far walls of the common carotid artery, carotid bifurcation, and internal carotid artery. A standardized protocol was used at all sites,[35,126] and measurements of carotid artery focal plaque, a marker of subclinical atherosclerosis, were obtained at a centralized reading center (U. of Southern California). Subclinical CVD (sCVD) was defined based on the presence of one or more carotid artery lesions.[35]

From the initial 1,865 participants in the WIHS vascular substudy, 32 participants were selected for scRNA-seq analysis. Because we were interested in the joint relationships of HIV infection and sCVD with surface marker and RNA expression by different cell subtypes, we used a two-by-two factorial design based on HIV, CVD and cholesterol treatment (mostly statins). CVD was defined as presence of carotid artery focal plaque at either vascular substudy visit to define four

groups of eight participants each: HIV-, HIV+CVD-, HIV+CVD+, HIV+CVD+ treated with cholesterol-lowering drugs. HIV infection status was ascertained by enzyme-linked immunosorbent assay (ELISA) and confirmed by Western blot. CVD participants either had one or more plaques at each vascular substudy visit, or more than one plaque at a single visit. Non-CVD participants with self-reported coronary heart disease or current lipid-lowering therapy use were excluded. Participants were formed in quartets matched by race/ethnicity (except one quartet), age (± 5 years) at the baseline vascular substudy (except one quartet where the age difference was more but all the women were post-menopausal), visit number, smoking history, and date of specimen collection (within 1 year).

Demographic, clinical, and laboratory variables were assessed from the same study visit using standardized protocols. **Table S1** shows characteristics of the study population. The median age at the baseline study visit was 55 years, and 96% of participants were either of black race or Hispanic ethnicity. Most (86%) reported a history of smoking. Substance use was highly prevalent, with 43% of HIV+ and 50% of HIV- participants reporting either a history of injection drug use; current use of crack, cocaine, or heroin; or alcohol use (≥14 drinks per week). Among HIV+ participants, over 80% reported use of HAART at the time PBMCs were obtained, and 59% reported an undetectable HIV-1 RNA level. The median CD4+ T-cell count was 585 cells/μL (IQR 382-816) in HIV+ women without sCVD and 535 cells/μL (IQR 265-792) in HIV+ women with sCVD.

Preparation of PBMC samples for CITE-seq. To avoid batch effects, sixteen samples each were processed on the same day. PBMC tubes were thawed in a 37℃ water bath and tubes filled with 8 mL of complete RPMI-1640 solution (**Table S13**; cRPMI-1640 contains Human Serum Albumin, HEPES, Sodium pyruvate, MEM-NEAA, Penicillin-Streptomicyn, GlutaMax and

Mercaptoethanol). The tubes were centrifuged at 400 xg for 5 minutes and pellets resuspended in cold staining buffer (SB: 2 % fetal bovine serum (FBS) in in phosphate-buffered saline (PBS)). All reagents, manufacturers and catalogue numbers are listed in **Table S13**. Manual cell counting was performed by diluting cell concentration to achieve 100-400 cells per hemocytometer count. Cells were aliquoted to a count of 1 million cells each and incubated on ice with Fc Block (BD, **Table S13**) at a 1:20 dilution, centrifuged at 400 xg for 5 minutes, resuspended in 180 μL of SB and transferred to their respective sample Multiplexing Kit tubes (BD). The cells were incubated for 20 minutes at room temperature, transferred to 5 mL polystyrene tubes, washed with 3 mL SB and centrifuged at 400 xg for 5 minutes. The addition of 2 mL of SB to the tubes and centrifugation was repeated 2 more times for a total of 3 washes. The cells were resuspended in 400 μL of SB and 2 μL of DRAQ7 and Calcein AM were added to each tube. The viability and cell count of each tube was determined using the BD Rhapsody Scanner (Scanner) (**Table S2**). Tube contents were pooled in equal proportions with total cell counts not to exceed 1 million cells. The tubes were then centrifuged at 400 xg for 5 minutes and resuspended in a cocktail of 40 AbSeq antibodies (2 μL each and 20 μL of SB) on ice for 30-60 minutes per manufacturer's recommendations. The tubes were then washed with 2 mL of SB followed by centrifugation at 400 xg for 5 minutes. This was repeated two more times for a total of 3 washes. The cells were then counted again using the Scanner.

Library preparation. Cells were loaded at 800-1000 cells/μL into the primed plate. The plate was primed and then loaded and unloaded per the User Guide described by BD when using a Scanner. The lysis buffer that was collected was removed by having the beads isolated with a magnet and the supernatant removed. Reverse Transcription was performed at 37℃ on a thermomixer at 1200 rpm for 20 minutes. Exonuclease I was then incubated at 37℃ on a thermomixer at 1200 rpm for 30 minutes and then immediately placed on a heat block at 80℃ for 20 minutes. The tube

was placed on ice followed by supernatant removal while beads were on a magnet. The beads were resuspended in Bead Resuspension solution (provided in BD kit). Then, the tubes were stored in 4℃ until further processing. Per BD's protocol, the reagents for PCR1 including the BD Human Immune Response Panel and our custom panel of ~100 genes were added to the beads. Next samples were aliquoted into four 0.2 mL strip PCR tubes and incubated for 10 cycles according to BD's protocol for PCR1. A double size selection was performed using AMPure XPre beads at a ratio of 0.7X (RNA tube). The supernatant was transferred to a new tube and an additional 100 μL of AMPure XP beads were added (sample tags and antibodies). The RNA tube was washed twice with 500 μL of 80 % ethanol. 550 μl of supernatant were removed from the antibody tube followed by two washes with 500 μL of 80 % ethanol. The cDNA was eluted off the beads using 30 μL of BD elution buffer and then transferred to a 1.5mL tube.

Pre-sequencing quality control (QC). A QC/ quantification check was performed on the tube containing AbSeq and Sample Tags using Agilent TapeStation high sensitivity D1000 screentape. 5 μL from each tube (mRNA and Ab/ST) was then added to their respective tubes containing the reagents for PCR2. mRNA had the reagents required for amplifying the Human Immune Response Panel and the Custom panel, while the Sample Tags had the reagents required for amplifying them specifically. Each tube had 12 cycles of PCR performed according to BD' User Guide. Each tube was then cleaned with AMPure XP beads with the following ratios 0.8X for mRNA and 1.2X for ST. Two 200 μL washes were performed during the clean-up using 80 % ethanol per sample. The cDNA was eluted off using BD elution buffer. A QC/ quantification check was performed using Agilent TapeStation high sensitivity D1000 screen tape and Qubit double stranded high sensitivity DNA test kit. The mRNA was then diluted, if necessary, to a concentration of 1.2-2.7 ng/μL and the Ab/ST tube as well as the Sample Tag library from PCR2 were diluted, if needed, to a concentration of 0.5-1.1 ng/μL. From each sample 3 μL were added

to a volume of 47 μL of reagents for PCR3 as described by BD's User Guide following the protocol and number of cycles listed, except for AbSeq, which had 9 cycles of PCR performed as described by previous optimization. The three libraries were then cleaned with AMPure XP beads at the following ratios: mRNA 0.7X AbSeq and Sample Tag 0.8X. Samples were washed twice with 200 μL of 80 % ethanol. The cDNA was eluted off the beads using BD's elution buffer. Then a final QC and quantification check was performed using TapeStation and Qubit kits and reagents.

Sequencing. The samples were pooled and sequenced to the following nominal depth recommended by BD: AbSeq: n x 1000 reads per cell, where n is the plexity of AbSeq used; mRNA: 20,000 reads per cell; Sample Tags: 600 reads per cell. A total of 60,600 reads per cell were desired for sequencing on the NovaSeq. The samples and specifications for pooling and sequencing depth, along with number of cells loaded onto each plate was optimized for S1 and S2 100 cycle kits (Illumina) with the configuration of 67x8x50 bp. Once sequencing was complete, a FASTA file was generated by BD as a reference for our AbSeq and genes we targeted with these assays. The FASTA file and FASTQ files generated by the NovaSeq were uploaded to Seven Bridged Genomics pipeline, where the data was filter in matrices and csv files. This analysis generated draft transcriptomes and surface phenotypes of 54,078 cells (496 genes, 40 antibodies). 11 genes were not expressed, i.e. had exactly 0 total reads in all cells combined. These genes were removed, leaving 485 genes for analysis.

Doublet Removal. Based on the 4 sample tags used per plate, 8,359 doublets were removed. The remaining 45,719 cells were analyzed using the Doublet Finder package on R (https://github.com/chris-mcginnis-ucsf/DoubletFinder) with the default doublet formation rate (7.5%). This removed another 3,322 doublets, leaving 42,397 Cells. Finally, we removed all cells that had less than 128 (2^7) antibody molecules sequenced. This removed 786 noisy cells, resulting

in 41,611 cell transcriptomes. All antibody data were CLR (centered log-ratio) normalized and converted to log2 scale. All transcripts were normalized by total UMIs in each cell and scaled up to 1000.

Identifying Major Cell Types by Biaxial Gating. To identify the major known cell types, we used antibodies to CD3, CD19, CD4, CD8, CD14, CD16 and CD56. Cell type definitions:

- B cells: CD19+ and CD3-
- T cells: CD19- and CD3+ as T cells. (To find CD4T and CD8T further ahead in the analysis)
- CD4 T cells: CD4+ and CD8- T cells
- CD 8 T cells: CD8+ and CD4- T cells
- Monocytes and NK cells from CD19-CD3- (non-B non-T cells)
- CM: CD14+CD16- (non-B non-T cells)
- INT: CD14+CD16+ (non-B non-T cells)
- NCM: CD14-CD16+CD56- (non-B non-T cells)
- NK: CD4- CD56+ CD14- CD20- CD123- CD206- (non-B non-T cells)

As is standard in the NK cell field,[127] the CD16- immature NK cells were gated to a higher level of CD56 as shown in figure S3. The mature NK cells were CD19-CD3-CD16+CD56+. One CD16+CD56- cluster was also identified as NK cells. This resulted in 2919 B cells, 11,045 CD4 T cells, 12,843 CD8 T cells, 5,145 CM, 1009 INT, 475 NCM and 1,843 NK cells.

Thresholding. Each antibody threshold (**Table S5**) was obtained by determining its expression in a known negative cell. To identify the thresholds, biaxial plots of mutually exclusive markers were used to best separate the positive populations from the noise. In combined protein and

transcript panel single cell sequencing, non-specific background staining is caused by incomplete Fc block and oligonucleotide-tagged antibody being trapped in the nanowell.[49]

Clustering. Clustering was performed using UMAP (Uniform Manifold Approximation and Projection) and Louvain clustering.[72] UMAP is a manifold learning technique for dimensionality reduction. It is based on the neighborhood graphs, which captures the local relationship in the data. UMAP is able to maintain local structure and also preserve global distances in the reduced dimension, i.e the cells that are similar in the high dimension remain close-by in the 2 dimensions and the cells that different are apart in the 2 dimensions. There are a few parameters that define the dimensionality reduction when using UMAP; 1) N_neighbours: This is used to create the neighborhood graph. It controls how the UMAP balances the local and the global structure. It gives the size of the local neighborhood the algorithm looks at while trying to obtain the lower dimensional manifold. Larger values give a more global view while smaller values give more on local view. 2) n_pcs: This gives the number of principal components of the data to consider while creating the neighborhood graph. 3) min_dist: This parameter provides the minimum distance between embedded points. Smaller values result in more dense embedding while larger values result in a more spread-out embedding. 4) Spread: This parameter determines the scale at which the points are spread out. Together with min_dist, it determines the closeness of points in the cluster. The clustering parameters used were: n_neighbors = 100, n_pcs = 50, min_dist = 1, spread = 1, random state = 42. Louvain resolution was set at 0.8. Subclustering of each major cell type was based on all non-negative antibodies (**Table S7**).

Cluster Assignment. Louvain clusters produced 12 clusters with clearly bimodal expression of at least one cell surface marker. In CD4 T cell, 4 of the initial clusters were further divided based on the expression of CD11c, CD56, CD25, CD127, CXCR3 and CCR2. CD8 T cells had two clusters that were divided based on CD11c, CD16 and CXCR3 surface marker expression. One

cluster from classical monocytes and one cluster from intermediate monocytes were further divided based on CCR7 and CD152 expression, respectively. In non-classical monocytes, one cluster showed differential expression of CD36 and CD152 surface marker expression and was divided in two. In B cells, one cluster was split because it showed differential expression of CD25 and CXCR3 within the cluster. Finally, two clusters from NK cells were split due to CD16, CD56 and CD11c expression.

Comparing Gene Expression among Participant Types. To determine differential expression (DE) among the four types of participants, we use the Seurat package in R with no thresholds over avg_logFC, minimum fraction of cells required in the two populations being compared, minimum number of cells and minimum number of cells expressing a feature in either group. We filtered for adjusted $p<0.05$ and compared HIV-, HIV+CVD-, HIV+CVD+ and HIV+CVD+ statin-treated. From this data, volcano plots were generated using ggplot2 and ggrepel packages in R, Axis were restricted to the range of (-2,2) on the x-axis and (0,20) on the y-axis. Genes outside these ranges were bounded to the corresponding limit of the axes.

Comparing Cell Proportions. To find changes in proportions, we identified the cell numbers for each participant in each cluster (**Table S4)**. Statistical differences in cell proportions were calculated by log-odds ratio defined as p/(1-p) where p is the proportion of cells, followed by ANOVA and Tukey's multiple comparison test between the four groups. For clarity, the data is presented as percentage of cells.

Correlation Analysis. We correlated each antibody to its corresponding gene(s) using Spearman rank correlation and significance (R package). For each combination of gene-antibody, we discarded cells that had values below the corresponding threshold for that antibody as well as cells with zero counts for that gene. After this filter, any gene-antibody combination that had 10

cells or less was deemed insignificant. Finally, all non-significant (p-value > 0.05) were designated a nominal value of zero as the Spearman rank correlation coefficient and we selected only those genes or antibodies that had at least one correlation whose coefficient >= 0.25 or whose coefficient <= -0.25. All significant non-negative correlations are reported in **Table S6**.

Authors

Jenifer Vallejo,[1#] Ryosuke Saigusa,[1#] Rishab Gulati,[1] Yanal Ghosheh,[1] Christopher P. Durant,[1] Payel Roy,[1] Erik Ehinger,[1] Tanyaporn Pattarabanjird,[2] Lindsey E. Padgett,[1] Claire E. Olingy,[1] David B. Hanna,[3] Alan L. Landay,[4] Russell P. Tracy,[5] Jason M. Lazar,[6] Wendy J. Mack,[7,8] Kathleen M. Weber,[9] Adaora A. Adimora,[10] Howard N. Hodis,[7,8] Phyllis C. Tien,[11] Igho Ofotokun,[12] Sonya L. Heath,[13] Huy Q. Dinh,[1] Avishai Shemesh,[14] Coleen A. McNamara,[2] Lewis L. Lanier,[14] Catherine C. Hedrick,[1] Robert C. Kaplan,[3,15] Klaus Ley.[1,16*]

[1]La Jolla Institute for Immunology, La Jolla, CA, USA.

[2]Cardiovascular Research Center, Cardiovascular Division, Department of Medicine, University of Virginia, Charlottesville.

[3]Albert Einstein College of Medicine, Department of Epidemiology and Population Health, Bronx, NY, USA.

[4]Rush University Medical Center, Department of Internal Medicine, Chicago, IL, USA.

[5]University of Vermont Larner College of Medicine, Departments of Pathology & Laboratory Medicine and Biochemistry, Colchester, VT, USA.

[6]SUNY Downstate Health Sciences University, Department of Medicine, Brooklyn, NY, USA.

[7]Keck School of Medicine, University of Southern California, Department of Preventive Medicine, Los Angeles, CA, USA.

[8]Atherosclerosis Research Unit, University of Southern California, Los Angeles, CA, USA.

[9]Cook County Health/Hektoen Institute of Medicine, Chicago, IL, USA.

[10]Department of Medicine, University of North Carolina School of Medicine, The University of North Carolina at Chapel Hill, Chapel Hill, North Carolina.

[11]Department of Medicine, University of California, San Francisco, San Francisco, CA and Department of Veterans Affairs Medical Center, San Francisco, CA, USA.

[12]Emory University School of Medicine, Department of Medicine, Infectious Disease Division and Grady Health Care System, Atlanta, GA, USA.

[13]University of Alabama at Birmingham, Department of Medicine, Birmingham, AL, USA.

[14]Parker Institute for Cancer Immunotherapy, University of California, San Francisco, CA, USA; Department of Microbiology and Immunology, University of California, San Francisco, CA, USA.

[15] Fred Hutchinson Cancer Research Center, Public Health Sciences Division, Seattle, WA, USA.

[16] University of California San Diego, San Diego, CA, USA.

Acknowledgements

Supported by R35-HL-145241, R01-HL-121697, R01-HL-148094 to K.L., P01-KL-136275, R01-HL-134236 to C.C.H., R01-HL-126543, 5R01-HL-126543-05, 5R01-HL-140976-02, 1R01-HL-148094-01, R01-HL-148094 to R.C.K., K01-HL-137557 to D.B.H., U01-AI-103408 to I.O., U01-AI-103390 to A.A.A., U01-AI-034989 to P.C.T., Cancer Research Institute (CRI) to A.S., AHA-19POST34450020 to L.E.P, NIAID, NICHD, NCI, NIDA, NIMH, NIDCR, NIAAA, NIDCD, UL1-TR-000004, P30-AI-050409, P30-AI-050410, and P30-AI-027767. Data in this manuscript were collected by the Womens Interagency HIV study, now the MACS/WIHS Combined Cohort Study (MWCCS).

Conflict of interest

There are no conflicts of interest.

Author contribution

J.V., R.S., Y.G., C.P.D., E.E., and K.L. designed the study. A.L.L., R.P.T., J.M.L., W.J.M., K.M.W, A.A.A., H.N.H., P.C.T., I.O., S.L.H., and R.C.K., collected samples and data. D.B.H. analyzed clinical data. H.N.H. designed and collected data for the B mode ultrasound substudy. C.P.D., and E.E. ran the scRNA-Seq experiments. J.V., R.S., R.G., Y.G., P.R., T.P., L.E.P., C.E.O., H.Q.D., A.A., C.A.M., L.L.L., C.C.H., and K.L analyzed the data. R.G., Y.G. and H.Q.D. conducted the bioinformatics analysis. J.V., R.S., and K.L. wrote the manuscript.

References

1. Montaner JSG, Lima VD, Harrigan PR, et al. Expansion of HAART coverage is associated with sustained decreases in HIV/AIDS morbidity, mortality and HIV transmission: the "HIV Treatment as Prevention" experience in a Canadian setting. *PLoS One*. 2014;9(2):e87872. doi:10.1371/journal.pone.0087872
2. Hanna DB, Lin J, Post WS, et al. Association of Macrophage Inflammation Biomarkers With Progression of Subclinical Carotid Artery Atherosclerosis in HIV-Infected Women and Men. *J Infect Dis*. 2017;215(9):1352-1361. doi:10.1093/infdis/jix082
3. Mocroft A, Reiss P, Gasiorowski J, et al. Serious fatal and nonfatal non-AIDS-defining illnesses in Europe. *J Acquir Immune Defic Syndr*. 2010;55(2):262-270. doi:10.1097/QAI.0b013e3181e9be6b
4. Neuhaus J, Angus B, Kowalska JD, et al. Risk of all-cause mortality associated with nonfatal AIDS and serious non-AIDS events among adults infected with HIV. *AIDS*. 2010;24(5):697-706. doi:10.1097/QAD.0b013e3283365356
5. Saves M, Chene G, Ducimetiere P, et al. Risk factors for coronary heart disease in patients treated for human immunodeficiency virus infection compared with the general population. *Clin Infect Dis*. 2003;37(2):292-298. doi:10.1086/375844
6. Kaplan RC, Kingsley LA, Sharrett AR, et al. Ten-year predicted coronary heart disease risk in HIV-infected men and women. *Clin Infect Dis*. 2007;45(8):1074-1081. doi:10.1086/521935
7. Smit M, Brinkman K, Geerlings S, et al. Future challenges for clinical care of an ageing population infected with HIV: a modelling study. *Lancet Infect Dis*. 2015;15(7):810-818. doi:10.1016/S1473-3099(15)00056-0
8. Twigg HL 3rd, Crystal R, Currier J, et al. Refining Current Scientific Priorities and Identifying New Scientific Gaps in HIV-Related Heart, Lung, Blood, and Sleep Research. *AIDS Res*

Hum Retroviruses. 2017;33(9):889-897. doi:10.1089/AID.2017.0026

9. Deeks SG, Overbaugh J, Phillips A, Buchbinder S. HIV infection. *Nat Rev Dis Prim*. 2015;1:15035. doi:10.1038/nrdp.2015.35

10. Le T, Wright EJ, Smith DM, et al. Enhanced CD4+ T-cell recovery with earlier HIV-1 antiretroviral therapy. *N Engl J Med*. 2013;368(3):218-230. doi:10.1056/NEJMoa1110187

11. Milush JM, Lopez-Verges S, York VA, et al. CD56negCD16(+) NK cells are activated mature NK cells with impaired effector function during HIV-1 infection. *Retrovirology*. 2013;10:158. doi:10.1186/1742-4690-10-158

12. Mueller KAL, Hanna DB, Ehinger E, et al. Loss of CXCR4 on non-classical monocytes in participants of the Women's Interagency HIV Study (WIHS) with subclinical atherosclerosis. *Cardiovasc Res*. 2019;115(6):1029-1040. doi:10.1093/cvr/cvy292

13. Baker J V, Hullsiek KH, Singh A, et al. Immunologic predictors of coronary artery calcium progression in a contemporary HIV cohort. *AIDS*. 2014;28(6):831-840. doi:10.1097/QAD.0000000000000145

14. Schechter ME, Andrade BB, He T, et al. Inflammatory monocytes expressing tissue factor drive SIV and HIV coagulopathy. *Sci Transl Med*. 2017;9(405). doi:10.1126/scitranslmed.aam5441

15. Ehinger E, Ghosheh Y, Bala PA, et al. Classical Monocyte Transcriptomes Reveal Significant Anti- Inflammatory Statin Effect in Women with Chronic HIV. *Cardiovasc Res*. Forthcomin.

16. Cooper MA, Fehniger TA, Caligiuri MA. The biology of human natural killer-cell subsets. *Trends Immunol*. 2001;22(11):633-640. doi:10.1016/s1471-4906(01)02060-9

17. Cooper MA, Fehniger TA, Turner SC, et al. Human natural killer cells: a unique innate immunoregulatory role for the CD56(bright) subset. *Blood*. 2001;97(10):3146-3151. doi:10.1182/blood.v97.10.3146

18. Jacobs R, Hintzen G, Kemper A, et al. CD56bright cells differ in their KIR repertoire and

cytotoxic features from CD56dim NK cells. *Eur J Immunol*. 2001;31(10):3121-3127. doi:10.1002/1521-4141(2001010)31:10<3121::aid-immu3121>3.0.co;2-4

19. Smith SL, Kennedy PR, Stacey KB, et al. Diversity of peripheral blood human NK cells identified by single-cell RNA sequencing. *Blood Adv*. 2020;4(7):1388-1406. doi:10.1182/bloodadvances.2019000699

20. Hu PF, Hultin LE, Hultin P, et al. Natural killer cell immunodeficiency in HIV disease is manifest by profoundly decreased numbers of CD16+CD56+ cells and expansion of a population of CD16dimCD56- cells with low lytic activity. *J Acquir Immune Defic Syndr Hum Retrovirol*. 1995;10(3):331-340.

21. Mavilio D, Lombardo G, Benjamin J, et al. Characterization of CD56-/CD16+ natural killer (NK) cells: a highly dysfunctional NK subset expanded in HIV-infected viremic individuals. *Proc Natl Acad Sci U S A*. 2005;102(8):2886-2891. doi:10.1073/pnas.0409872102

22. Gonzalez VD, Falconer K, Michaelsson J, et al. Expansion of CD56- NK cells in chronic HCV/HIV-1 co-infection: reversion by antiviral treatment with pegylated IFNalpha and ribavirin. *Clin Immunol*. 2008;128(1):46-56. doi:10.1016/j.clim.2008.03.521

23. Phillips AN, Sabin CA, Elford J, Bofill M, Lee CA, Janossy G. CD8 lymphocyte counts and serum immunoglobulin A levels early in HIV infection as predictors of CD4 lymphocyte depletion during 8 years of follow-up. *AIDS*. 1993;7(7):975-980. doi:10.1097/00002030-199307000-00011

24. Badejo OA, Chang C-C, So-Armah KA, et al. CD8+ T-cells count in acute myocardial infarction in HIV disease in a predominantly male cohort. *Biomed Res Int*. 2015;2015:246870. doi:10.1155/2015/246870

25. Overton ET, Sterrett S, Westfall AO, et al. Effects of atorvastatin and pravastatin on immune activation and T-cell function in antiretroviral therapy-suppressed HIV-1-infected patients. *AIDS*. 2014;28(17):2627-2631. doi:10.1097/QAD.0000000000000475

26. Eckard AR, Meissner EG, Singh I, McComsey GA. Cardiovascular Disease, Statins, and

HIV. *J Infect Dis*. 2016;214 Suppl(Suppl 2):S83-92. doi:10.1093/infdis/jiw288

27. Griffin DO, Rothstein TL. Human b1 cell frequency: isolation and analysis of human b1 cells. *Front Immunol*. 2012;3:122. doi:10.3389/fimmu.2012.00122

28. Upadhye A, Srikakulapu P, Gonen A, et al. Diversification and CXCR4-Dependent Establishment of the Bone Marrow B-1a Cell Pool Governs Atheroprotective IgM Production Linked to Human Coronary Atherosclerosis. *Circ Res*. 2019;125(10):e55-e70. doi:10.1161/CIRCRESAHA.119.315786

29. Tanigawa T, Kitamura A, Yamagishi K, et al. Relationships of differential leukocyte and lymphocyte subpopulations with carotid atherosclerosis in elderly men. *J Clin Immunol*. 2003;23(6):469-476. doi:10.1023/b:joci.0000010423.65719.e5

30. Moir S, Fauci AS. B-cell responses to HIV infection. *Immunol Rev*. 2017;275(1):33-48. doi:10.1111/imr.12502

31. Moir S, Fauci AS. B cells in HIV infection and disease. *Nat Rev Immunol*. 2009;9(4):235-245. doi:10.1038/nri2524

32. Karnell JL, Kumar V, Wang J, Wang S, Voynova E, Ettinger R. Role of CD11c(+) T-bet(+) B cells in human health and disease. *Cell Immunol*. 2017;321:40-45. doi:10.1016/j.cellimm.2017.05.008

33. Guillaumet-Adkins A, Rodriguez-Esteban G, Mereu E, et al. Single-cell transcriptome conservation in cryopreserved cells and tissues. *Genome Biol*. 2017;18(1):45. doi:10.1186/s13059-017-1171-9

34. Williams JW, Winkels H, Durant CP, Zaitsev K, Ghosheh Y, Ley K. Single Cell RNA Sequencing in Atherosclerosis. *Circ Res*. 2020;126(9):1112-1126. doi:10.1161/CIRCRESAHA.119.315940

35. Kaplan RC, Kingsley LA, Gange SJ, et al. Low CD4+ T-cell count as a major atherosclerosis risk factor in HIV-infected women and men. *AIDS*. 2008;22(13):1615-1624. doi:10.1097/QAD.0b013e328300581d

36. Hanna DB, Post WS, Deal JA, et al. HIV Infection Is Associated With Progression of Subclinical Carotid Atherosclerosis. *Clin Infect Dis*. 2015;61(4):640-650. doi:10.1093/cid/civ325

37. Hodis HN, Mack WJ, Lobo RA, et al. Estrogen in the prevention of atherosclerosis. A randomized, double-blind, placebo-controlled trial. *Ann Intern Med*. 2001;135(11):939-953. doi:10.7326/0003-4819-135-11-200112040-00005

38. Zheng C, Zheng L, Yoo J-K, et al. Landscape of Infiltrating T Cells in Liver Cancer Revealed by Single-Cell Sequencing. *Cell*. 2017;169(7):1342-1356.e16. doi:10.1016/j.cell.2017.05.035

39. Zhang Y, Zheng L, Zhang L, Hu X, Ren X, Zhang Z. Deep single-cell RNA sequencing data of individual T cells from treatment-naive colorectal cancer patients. *Sci data*. 2019;6(1):131. doi:10.1038/s41597-019-0131-5

40. Zhang L, Li Z, Skrzypczynska KM, et al. Single-Cell Analyses Inform Mechanisms of Myeloid-Targeted Therapies in Colon Cancer. *Cell*. 2020;181(2):442-459.e29. doi:10.1016/j.cell.2020.03.048

41. Brown CC, Gudjonson H, Pritykin Y, et al. Transcriptional Basis of Mouse and Human Dendritic Cell Heterogeneity. *Cell*. 2019;179(4):846-863.e24. doi:10.1016/j.cell.2019.09.035

42. Uniken Venema WT, Voskuil MD, Vila AV, et al. Single-Cell RNA Sequencing of Blood and Ileal T Cells From Patients With Crohn's Disease Reveals Tissue-Specific Characteristics and Drug Targets. *Gastroenterology*. 2019;156(3):812-815.e22. doi:10.1053/j.gastro.2018.10.046

43. Martin JC, Chang C, Boschetti G, et al. Single-Cell Analysis of Crohn's Disease Lesions Identifies a Pathogenic Cellular Module Associated with Resistance to Anti-TNF Therapy. *Cell*. 2019;178(6):1493-1508.e20. doi:10.1016/j.cell.2019.08.008

44. Reyes M, Vickers D, Billman K, et al. Multiplexed enrichment and genomic profiling of

peripheral blood cells reveal subset-specific immune signatures. *Sci Adv*. 2019;5(1):eaau9223. doi:10.1126/sciadv.aau9223

45. Kotliarov Y, Sparks R, Martins AJ, et al. Broad immune activation underlies shared set point signatures for vaccine responsiveness in healthy individuals and disease activity in patients with lupus. *Nat Med*. 2020. doi:10.1038/s41591-020-0769-8

46. Kazer SW, Aicher TP, Muema DM, et al. Integrated single-cell analysis of multicellular immune dynamics during hyperacute HIV-1 infection. *Nat Med*. 2020;26(4):511-518. doi:10.1038/s41591-020-0799-2

47. Fan HC, Fu GK, Fodor SPA. Expression profiling. Combinatorial labeling of single cells for gene expression cytometry. *Science*. 2015;347(6222). doi:10.1126/science.1258367

48. Mair F, Erickson JR, Voillet V, et al. A Targeted Multi-omic Analysis Approach Measures Protein Expression and Low-Abundance Transcripts on the Single-Cell Level. *Cell Rep*. 2020;31(1):107499. doi:10.1016/j.celrep.2020.03.063

49. Stoeckius M, Hafemeister C, Stephenson W, et al. Simultaneous epitope and transcriptome measurement in single cells. *Nat Methods*. 2017;14(9):865-868. doi:10.1038/nmeth.4380

50. Peterson VM, Zhang KX, Kumar N, et al. Multiplexed quantification of proteins and transcripts in single cells. *Nat Biotechnol*. 2017;35(10):936-939. doi:10.1038/nbt.3973

51. Biburger M, Trenkwald I, Nimmerjahn F. Three blocks are not enough--Blocking of the murine IgG receptor FcγRIV is crucial for proper characterization of cells by FACS analysis. *Eur J Immunol*. 2015;45(9):2694-2697. doi:10.1002/eji.201545463

52. Andersen MN, Al-Karradi SNH, Kragstrup TW, Hokland M. Elimination of erroneous results in flow cytometry caused by antibody binding to Fc receptors on human monocytes and macrophages. *Cytometry A*. 2016;89(11):1001-1009. doi:10.1002/cyto.a.22995

53. Ravetch J V, Clynes RA. Divergent roles for Fc receptors and complement in vivo. *Annu Rev Immunol*. 1998;16:421-432. doi:10.1146/annurev.immunol.16.1.421

54. Ravetch J V. Fc receptors. *Curr Opin Immunol*. 1997;9(1):121-125. doi:10.1016/s0952-7915(97)80168-9

55. Ravetch J V, Bolland S. IgG Fc receptors. *Annu Rev Immunol*. 2001;19:275-290. doi:10.1146/annurev.immunol.19.1.275

56. Nimmerjahn F, Ravetch J V. Fc-Receptors as Regulators of Immunity. *Adv Immunol*. 2007;96:179-204. doi:10.1016/S0065-2776(07)96005-8

57. Butler A, Hoffman P, Smibert P, Papalexi E, Satija R. Integrating single-cell transcriptomic data across different conditions, technologies, and species. *Nat Biotechnol*. 2018;36(5):411-420. doi:10.1038/nbt.4096

58. Stuart T, Butler A, Hoffman P, et al. Comprehensive Integration of Single-Cell Data. *Cell*. 2019;177(7):1888-1902.e21. doi:10.1016/j.cell.2019.05.031

59. Winkels H, Ehinger E, Vassallo M, et al. Atlas of the immune cell repertoire in mouse atherosclerosis defined by single-cell RNA-sequencing and mass cytometry. *Circ Res*. 2018;122(12):1675-1688. doi:10.1161/CIRCRESAHA.117.312513

60. Cole JE, Park I, Ahern DJ, et al. Immune cell census in murine atherosclerosis: cytometry by time of flight illuminates vascular myeloid cell diversity. *Cardiovasc Res*. 2018;114(10):1360-1371. doi:10.1093/cvr/cvy109

61. Spitzer MH, Nolan GP. Mass Cytometry: Single Cells, Many Features. *Cell*. 2016;165(4):780-791. doi:10.1016/j.cell.2016.04.019

62. Robinson JP, Roederer M. HISTORY OF SCIENCE. Flow cytometry strikes gold. *Science*. 2015;350(6262):739-740. doi:10.1126/science.aad6770

63. Liu Y, Beyer A, Aebersold R. On the Dependency of Cellular Protein Levels on mRNA Abundance. *Cell*. 2016;165(3):535-550. doi:10.1016/j.cell.2016.03.014

64. Lundberg E, Fagerberg L, Klevebring D, et al. Defining the transcriptome and proteome in three functionally different human cell lines. *Mol Syst Biol*. 2010;6:450. doi:10.1038/msb.2010.106

65. Cochain C, Vafadarnejad E, Arampatzi P, et al. Single-Cell RNA-Seq Reveals the Transcriptional Landscape and Heterogeneity of Aortic Macrophages in Murine Atherosclerosis. *Circ Res*. 2018;122(12):1661-1674. doi:10.1161/CIRCRESAHA.117.312509

66. Ong S-M, Teng K, Newell E, et al. A Novel, Five-Marker Alternative to CD16-CD14 Gating to Identify the Three Human Monocyte Subsets. *Front Immunol*. 2019;10:1761. doi:10.3389/fimmu.2019.01761

67. Spear TT, Nishimura MI, Simms PE. Comparative exploration of multidimensional flow cytometry software: a model approach evaluating T cell polyfunctional behavior. *J Leukoc Biol*. 2017;102(2):551-561. doi:10.1189/jlb.6A0417-140R

68. Bryceson YT, Fauriat C, Nunes JM, et al. Functional analysis of human NK cells by flow cytometry. *Methods Mol Biol*. 2010;612:335-352. doi:10.1007/978-1-60761-362-6_23

69. Hong HS, Eberhard JM, Keudel P, et al. Phenotypically and functionally distinct subsets contribute to the expansion of CD56-/CD16+ natural killer cells in HIV infection. *AIDS*. 2010;24(12):1823-1834. doi:10.1097/QAD.0b013e32833b556f

70. Gregson JNS, Kuri-Cervantes L, Mela CM, Gazzard BG, Bower M, Goodier MR. Short communication: NKG2C+ NK cells contribute to increases in CD16+CD56- cells in HIV type 1+ individuals with high plasma viral load. *AIDS Res Hum Retroviruses*. 2013;29(1):84-88. doi:10.1089/AID.2011.0397

71. Spits H, Bernink JH, Lanier L. NK cells and type 1 innate lymphoid cells: partners in host defense. *Nat Immunol*. 2016;17(7):758-764. doi:10.1038/ni.3482

72. Subelj L, Bajec M. Unfolding communities in large complex networks: combining defensive and offensive label propagation for core extraction. *Phys Rev E Stat Nonlin Soft Matter Phys*. 2011;83(3 Pt 2):36103. doi:10.1103/PhysRevE.83.036103

73. Hartigan-O'Connor DJ, Poon C, Sinclair E, McCune JM. Human CD4+ regulatory T cells express lower levels of the IL-7 receptor alpha chain (CD127), allowing consistent

identification and sorting of live cells. *J Immunol Methods*. 2007;319(1-2):41-52. doi:10.1016/j.jim.2006.10.008

74. Staats J. Immunophenotyping of Human Regulatory T Cells. *Methods Mol Biol*. 2019;2032:141-177. doi:10.1007/978-1-4939-9650-6_9

75. Acosta-Rodriguez E V, Rivino L, Geginat J, et al. Surface phenotype and antigenic specificity of human interleukin 17-producing T helper memory cells. *Nat Immunol*. 2007;8(6):639-646. doi:10.1038/ni1467

76. Emoto M, Zerrahn J, Miyamoto M, Perarnau B, Kaufmann SH. Phenotypic characterization of CD8(+)NKT cells. *Eur J Immunol*. 2000;30(8):2300-2311. doi:10.1002/1521-4141(2000)30:8<2300::AID-IMMU2300>3.0.CO;2-2

77. Seregin SS, Chen GY, Laouar Y. Dissecting CD8+ NKT Cell Responses to Listeria Infection Reveals a Component of Innate Resistance. *J Immunol*. 2015;195(3):1112-1120. doi:10.4049/jimmunol.1500084

78. Hamers AAJ, Dinh HQ, Thomas GD, et al. Human Monocyte Heterogeneity as Revealed by High-Dimensional Mass Cytometry. *Arterioscler Thromb Vasc Biol*. 2019;39(1):25-36. doi:10.1161/ATVBAHA.118.311022

79. SahBandar IN, Ndhlovu LC, Saiki K, et al. Relationship between Circulating Inflammatory Monocytes and Cardiovascular Disease Measures of Carotid Intimal Thickness. *J Atheroscler Thromb*. 2020;27(5):441-448. doi:10.5551/jat.49791

80. Ruiz-Limon P, Ortega-Castro R, Barbarroja N, et al. Molecular Characterization of Monocyte Subsets Reveals Specific and Distinctive Molecular Signatures Associated With Cardiovascular Disease in Rheumatoid Arthritis. *Front Immunol*. 2019;10:1111. doi:10.3389/fimmu.2019.01111

81. Rossol M, Kraus S, Pierer M, Baerwald C, Wagner U. The CD14(bright) CD16+ monocyte subset is expanded in rheumatoid arthritis and promotes expansion of the Th17 cell population. *Arthritis Rheum*. 2012;64(3):671-677. doi:10.1002/art.33418

82. Rogacev KS, Cremers B, Zawada AM, et al. CD14++CD16+ monocytes independently predict cardiovascular events: a cohort study of 951 patients referred for elective coronary angiography. *J Am Coll Cardiol*. 2012;60(16):1512-1520. doi:10.1016/j.jacc.2012.07.019

83. Tsukamoto M, Seta N, Yoshimoto K, Suzuki K, Yamaoka K, Takeuchi T. CD14(bright)CD16+ intermediate monocytes are induced by interleukin-10 and positively correlate with disease activity in rheumatoid arthritis. *Arthritis Res Ther*. 2017;19(1):28. doi:10.1186/s13075-016-1216-6

84. Han J, Wang B, Han N, et al. CD14(high)CD16(+) rather than CD14(low)CD16(+) monocytes correlate with disease progression in chronic HIV-infected patients. *J Acquir Immune Defic Syndr*. 2009;52(5):553-559. doi:10.1097/qai.0b013e3181c1d4fe

85. Ellery PJ, Tippett E, Chiu Y-L, et al. The CD16+ monocyte subset is more permissive to infection and preferentially harbors HIV-1 in vivo. *J Immunol*. 2007;178(10):6581-6589. doi:10.4049/jimmunol.178.10.6581

86. Tapp LD, Shantsila E, Wrigley BJ, Pamukcu B, Lip GYH. The CD14++CD16+ monocyte subset and monocyte-platelet interactions in patients with ST-elevation myocardial infarction. *J Thromb Haemost*. 2012;10(7):1231-1241. doi:10.1111/j.1538-7836.2011.04603.x

87. Wrigley BJ, Shantsila E, Tapp LD, Lip GYH. CD14++CD16+ monocytes in patients with acute ischaemic heart failure. *Eur J Clin Invest*. 2013;43(2):121-130. doi:10.1111/eci.12023

88. Narasimhan PB, Marcovecchio P, Hamers AAJ, Hedrick CC. Nonclassical Monocytes in Health and Disease. *Annu Rev Immunol*. 2019;37:439-456. doi:10.1146/annurev-immunol-042617-053119

89. Kaminski DA, Wei C, Qian Y, Rosenberg AF, Sanz I. Advances in human B cell phenotypic profiling. *Front Immunol*. 2012;3:302. doi:10.3389/fimmu.2012.00302

90. Amu S, Tarkowski A, Dorner T, Bokarewa M, Brisslert M. The human immunomodulatory

CD25+ B cell population belongs to the memory B cell pool. *Scand J Immunol*. 2007;66(1):77-86. doi:10.1111/j.1365-3083.2007.01946.x

91. Moir S, Ho J, Malaspina A, et al. Evidence for HIV-associated B cell exhaustion in a dysfunctional memory B cell compartment in HIV-infected viremic individuals. *J Exp Med*. 2008;205(8):1797-1805. doi:10.1084/jem.20072683

92. Krämer A, Green J, Pollard JJ, Tugendreich S. Causal analysis approaches in Ingenuity Pathway Analysis. *Bioinformatics*. 2014;30(4):523-530. doi:10.1093/bioinformatics/btt703

93. Nakayama M, Niki Y, Kawasaki T, et al. IL-32-PAR2 axis is an innate immunity sensor providing alternative signaling for LPS-TRIF axis. *Sci Rep*. 2013;3:2960. doi:10.1038/srep02960

94. Damen MSMA, Popa CD, Netea MG, Dinarello CA, Joosten LAB. Interleukin-32 in chronic inflammatory conditions is associated with a higher risk of cardiovascular diseases. *Atherosclerosis*. 2017;264:83-91. doi:10.1016/j.atherosclerosis.2017.07.005

95. Kim S-H, Han S-Y, Azam T, Yoon D-Y, Dinarello CA. Interleukin-32: a cytokine and inducer of TNFalpha. *Immunity*. 2005;22(1):131-142. doi:10.1016/j.immuni.2004.12.003

96. Virani SS, Nambi V, Hoogeveen R, et al. Relationship between circulating levels of RANTES (regulated on activation, normal T-cell expressed, and secreted) and carotid plaque characteristics: the Atherosclerosis Risk in Communities (ARIC) Carotid MRI Study. *Eur Heart J*. 2011;32(4):459-468. doi:10.1093/eurheartj/ehq367

97. Mackay F, Schneider P, Rennert P, Browning J. BAFF AND APRIL: a tutorial on B cell survival. *Annu Rev Immunol*. 2003;21:231-264. doi:10.1146/annurev.immunol.21.120601.141152

98. Smulski CR, Eibel H. BAFF and BAFF-Receptor in B Cell Selection and Survival. *Front Immunol*. 2018;9:2285. doi:10.3389/fimmu.2018.02285

99. Ridker PM, Everett BM, Thuren T, et al. Antiinflammatory Therapy with Canakinumab for Atherosclerotic Disease. *N Engl J Med*. 2017;377(12):1119-1131.

doi:10.1056/NEJMoa1707914

100. Tobias PS, Curtiss LK. TLR2 in murine atherosclerosis. *Semin Immunopathol*. 2008;30(1):23-27. doi:10.1007/s00281-007-0102-3

101. Mullick AE, Tobias PS, Curtiss LK. Modulation of atherosclerosis in mice by Toll-like receptor 2. *J Clin Invest*. 2005;115(11):3149-3156. doi:10.1172/JCI25482

102. Mullick AE, Soldau K, Kiosses WB, Bell TA 3rd, Tobias PS, Curtiss LK. Increased endothelial expression of Toll-like receptor 2 at sites of disturbed blood flow exacerbates early atherogenic events. *J Exp Med*. 2008;205(2):373-383. doi:10.1084/jem.20071096

103. Matloubian M, David A, Engel S, Ryan JE, Cyster JG. A transmembrane CXC chemokine is a ligand for HIV-coreceptor Bonzo. *Nat Immunol*. 2000;1(4):298-304. doi:10.1038/79738

104. Zhao G, Wang S, Wang Z, et al. CXCR6 deficiency ameliorated myocardial ischemia/reperfusion injury by inhibiting infiltration of monocytes and IFN-γ-dependent autophagy. *Int J Cardiol*. 2013;168(2):853-862. doi:10.1016/j.ijcard.2012.10.022

105. Wang J-H, Su F, Wang S, et al. CXCR6 deficiency attenuates pressure overload-induced monocytes migration and cardiac fibrosis through downregulating TNF-α-dependent MMP9 pathway. *Int J Clin Exp Pathol*. 2014;7(10):6514-6523.

106. Bekele Y, Lakshmikanth T, Chen Y, et al. Mass cytometry identifies distinct CD4+ T cell clusters distinguishing HIV-1-infected patients according to antiretroviral therapy initiation. *JCI insight*. 2019;4(3). doi:10.1172/jci.insight.125442

107. Hearps AC, Maisa A, Cheng W-J, et al. HIV infection induces age-related changes to monocytes and innate immune activation in young men that persist despite combination antiretroviral therapy. *AIDS*. 2012;26(7):843-853. doi:10.1097/QAD.0b013e328351f756

108. Martin GE, Gouillou M, Hearps AC, et al. Age-associated changes in monocyte and innate immune activation markers occur more rapidly in HIV infected women. *PLoS One*. 2013;8(1):e55279. doi:10.1371/journal.pone.0055279

109. Liang H, Xie Z, Shen T. Monocyte activation and cardiovascular disease in HIV infection.

Cell Mol Immunol. 2017;14(12):960-962. doi:10.1038/cmi.2017.109

110. Funderburg NT, Zidar DA, Shive C, et al. Shared monocyte subset phenotypes in HIV-1 infection and in uninfected subjects with acute coronary syndrome. *Blood*. 2012;120(23):4599-4608. doi:10.1182/blood-2012-05-433946

111. Wildgruber M, Aschenbrenner T, Wendorff H, et al. The “Intermediate” CD14(++)CD16(+) monocyte subset increases in severe peripheral artery disease in humans. *Sci Rep*. 2016;6:39483. doi:10.1038/srep39483

112. Heine GH, Ulrich C, Seibert E, et al. CD14(++)CD16+ monocytes but not total monocyte numbers predict cardiovascular events in dialysis patients. *Kidney Int*. 2008;73(5):622-629. doi:10.1038/sj.ki.5002744

113. Rasool ST, Tang H, Wu J, et al. Increased level of IL-32 during human immunodeficiency virus infection suppresses HIV replication. *Immunol Lett*. 2008;117(2):161-167. doi:10.1016/j.imlet.2008.01.007

114. Toribio M, Fitch K V, Stone L, et al. Assessing statin effects on cardiovascular pathways in HIV using a novel proteomics approach: Analysis of data from INTREPID, a randomized controlled trial. *EBioMedicine*. 2018;35:58-66. doi:10.1016/j.ebiom.2018.08.039

115. Longenecker CT, Sattar A, Gilkeson R, McComsey GA. Rosuvastatin slows progression of subclinical atherosclerosis in patients with treated HIV infection. *AIDS*. 2016;30(14):2195-2203. doi:10.1097/QAD.0000000000001167

116. Hoffmann U, Lu MT, Olalere D, et al. Rationale and design of the Mechanistic Substudy of the Randomized Trial to Prevent Vascular Events in HIV (REPRIEVE): Effects of pitavastatin on coronary artery disease and inflammatory biomarkers. *Am Heart J*. 2019;212:1-12. doi:10.1016/j.ahj.2019.02.011

117. Oesterle A, Laufs U, Liao JK. Pleiotropic Effects of Statins on the Cardiovascular System. *Circ Res*. 2017;120(1):229-243. doi:10.1161/CIRCRESAHA.116.308537

118. Berry JD, Dyer A, Cai X, et al. Lifetime risks of cardiovascular disease. *N Engl J Med*.

2012;366(4):321-329. doi:10.1056/NEJMoa1012848

119. Barkan SE, Melnick SL, Preston-Martin S, et al. The Women's Interagency HIV Study. WIHS Collaborative Study Group. *Epidemiology*. 1998;9(2):117-125.

120. Olson NC, Doyle MF, Sitlani CM, et al. Associations of Innate and Adaptive Immune Cell Subsets With Incident Type 2 Diabetes Risk: The MESA Study. *J Clin Endocrinol Metab*. 2020;105(3). doi:10.1210/clinem/dgaa036

121. Clift IC. Diagnostic Flow Cytometry and the AIDS Pandemic. *Lab Med*. 2015;46(3):e59-64. doi:10.1309/LMKHW2C86ZJDRTFE

122. De Milito A. B lymphocyte dysfunctions in HIV infection. *Curr HIV Res*. 2004;2(1):11-21. doi:10.2174/1570162043485068

123. Bonaccorsi I, Spinelli D, Cantoni C, et al. Symptomatic Carotid Atherosclerotic Plaques Are Associated With Increased Infiltration of Natural Killer (NK) Cells and Higher Serum Levels of NK Activating Receptor Ligands. *Front Immunol*. 2019;10:1503. doi:10.3389/fimmu.2019.01503

124. Trapnell C, Pachter L, Salzberg SL. TopHat: discovering splice junctions with RNA-Seq. *Bioinformatics*. 2009;25(9):1105-1111. doi:10.1093/bioinformatics/btp120

125. Wang L, Wang S, Li W. RSeQC: quality control of RNA-seq experiments. *Bioinformatics*. 2012;28(16):2184-2185. doi:10.1093/bioinformatics/bts356

126. Robinson MD, McCarthy DJ, Smyth GK. edgeR: a Bioconductor package for differential expression analysis of digital gene expression data. *Bioinformatics*. 2010;26(1):139-140. doi:10.1093/bioinformatics/btp616

127. Milush JM, Long BR, Snyder-Cappione JE, et al. Functionally distinct subsets of human NK cells and monocyte/DC-like cells identified by coexpression of CD56, CD7, and CD4. *Blood*. 2009;114(23):4823-4831. doi:10.1182/blood-2009-04-216374

Supplemental figure legends

Figure S1. Study design overview. Three group comparisons (HIV effect, CVD effect and cholesterol lowering treatment effect) and main steps of analysis**.**

Figure S2. Unbiased UMAP clustering. All cells were clustered based on 462 genes and 40 antibody markers using Seurat, revealing B cells, monocytes, DCs, NK and T cells (left). The monocytes and DCs were re-clustered showing 3 classical, 2 intermediate and 4 nonclassical monocyte clusters, 1 DC and 1 monocyte-DC cluster (right).

Figure S3. Gating scheme (A) and biaxial dot plots (B-E) to identify major known cell types. PBMCs from 32 WIHS participants were hash-tagged and stained with 40 oligonucleotide-tagged mAbs (table S3). **(B) B cells** were defined as CD19+CD3- and T cells as CD19-CD3+. **(C) T cells** were identified as CD4 (CD4+CD8-) or CD8 (CD4-CD8+). **(D)** All CD19-CD3- cells were gated for CD14 and CD16, with CD14+CD16- cells being classical (CM) and CD14+CD16+ being intermediate (INT) monocytes. **(E)** The CD14-CD16+ cells from panel D contain NK cells, which were identified by CD56 and defined as CD56+CD14-CD20-CD123-CD206-. Most of the remaining CD56-CD16+ cells were nonclassical monocytes (NCM).

Figure S4. Rainbow plots of cell surface phenotype not shown in Figure 2. The expression level of each of the 40 antibody markers was color-coded from dark blue (=0, not expressed) to red (highest expression, log2 scale, as per color bar in each panel). **(A) CD4 T cells**, **(B) CD8 T cells**, **(C) Monocytes** (**Classical monocytes; CM**, **Intermediate monocytes; INT**, and **Nonclassical monocytes; NCM**), **(D) B cells**, **(E) NK cells**.

Figure S5. Antibody expression in all clusters. Violin plots for each of the 58 PBMC clusters. **(A) CD4+ T cells** (total of 16 clusters), **(B) CD8+T cells** (total of 14 clusters), **(C) Classical monocytes** (total of 6 clusters), **(D) Intermediate monocytes** (total of 5 clusters), **(E) Nonclassical monocytes** (total of 3 clusters), **(F) B cells** (total of 6 clusters), **(G) NK cells** (total of 6 clusters).

Figure S6. Pathway analysis. Ingenuity pathway analysis (IPA) was conducted on all clusters, filtered for the 21 pathways most relevant to HIV and CVD. Enrichment p values shown as a heat map from blue ($P<0.05$) to red ($p<10^{-10}$).

Figure S7. Remaining volcano plots not shown in Figure 7.

Supplemental Excel tables

Supplemental Excel Table S1. The data underlying Figure 4. Full gene expression matrix. **(A)** Average gene expression per cell in all clusters. **(B)** Log2 normalized gene expression. **(C-I)** Gene expression of each cell in each cell type, **(C)** CD4 T cells, **(D)** CD8 T cells, **(E)** Classical monocytes (CM), **(F)** Intermediate monocytes (INT), **(G)** Nonclassical monocytes (NCM), **(H)** B cells, **(I)** NK cells.

Supplemental Excel Table S2. The data underlying Figure 5. Differentially expressed genes [HIV-CVD- vs HIV+CVD-, HIV-CVD+ vs HIV+CVD+, HIV+CVD+ vs HIV+CVD+Statin (cholesterol lowering drugs)] compared in each cell cluster. First group (before the '+') against second group (after the '+'). gene: gene name, p_val: raw p value, avg_logFC: average log2 fold change, pct.1: the percentage of cells that express the gene in the first group, pct.2: the percentage of cells where the gene is detected in the second group, p_val_adj: adjusted p-value, based on Bonferroni correction using all genes in the dataset p value adjusted by Benjamini-Hochberg for multiple comparisons.

Supplemental Excel Table S3. The data underlying Figure 6. Significantly differentially expressed genes in each PBMC cluster among the 4 patient types [HIV-CVD-, HIV+CVD-, HIV+CVD+, HIV+CVD+Statin+ (cholesterol lowering drugs)]